

# Essential Role for Thymosin $\beta$ 4 in Regulating Vascular Smooth Muscle Cell Development and Vessel Wall Stability

Alex Rossdeutsch,\* Nicola Smart,\* Karina N. Dubé, Martin Turner, Paul R. Riley

**Rationale:** Compromised development of blood vessel walls leads to vascular instability that may predispose to aneurysm with risk of rupture and lethal hemorrhage. There is currently a lack of insight into developmental insults that may define the molecular and cellular characteristics of initiating and perpetrating factors in adult aneurismal disease.

**Objective:** To investigate a role for the actin-binding protein thymosin  $\beta$ 4 (T $\beta$ 4), previously shown to be proangiogenic, in mural cell development and vascular wall stability.

**Methods and Results:** Phenotypic analyses of both global and endothelial-specific loss-of-function T $\beta$ 4 mouse models revealed a proportion of T $\beta$ 4-null embryos with vascular hemorrhage coincident with a reduction in smooth muscle cell coverage of their developing vessels. Mechanistic studies revealed that extracellular T $\beta$ 4 can stimulate differentiation of mesodermal progenitor cells to a mature mural cell phenotype through activation of the transforming growth factor-beta (TGF $\beta$ ) pathway and that reduced TGF $\beta$  signaling correlates with the severity of hemorrhagic phenotype in T $\beta$ 4-null vasculature.

**Conclusions:** T $\beta$ 4 is a novel endothelial secreted trophic factor that functions synergistically with TGF $\beta$  to regulate mural cell development and vascular wall stability. These findings have important implications for understanding congenital anomalies that may be causative for adult-onset vascular instability. (*Circ Res.* 2012; 111:e89-e102.)

**Key Words:** thymosin ■ vasculature ■ mural cell ■ aorta ■ mouse ■ mouse mutants  
■ smooth muscle differentiation ■ vascular biology ■ vascular smooth muscle

The development of a functional vasculature is an essential process during embryogenesis, perturbations in which result in fetal lethality or vascular disease after birth. The formation of systemic blood vessels occurs in a stereotypical fashion -endothelial tubes form through a number of mechanisms (angiogenesis, vasculogenesis, or intussusception).<sup>1</sup> Endothelial cells then recruit mural cells comprising the subsets of vascular smooth muscle cells (VSMCs) and pericytes to the external wall of the vessel.<sup>2-4</sup> These mural cells are required to provide structural support for the blood vessel and probably play a role in maintaining endothelial health and integrity. The establishment of a vessel wall is accomplished either through the differentiation of de novo mural cells from precursor populations or recruitment from a proliferating pool

of mature cells. The former is thought to occur chiefly through the actions of endothelial secreted transforming growth factor-beta (TGF $\beta$ ) and the latter through paracrine platelet-derived growth factor-B (PDGF-B).<sup>4</sup> Typically, in the embryo, mural cells originate from the in situ differentiation of mesodermal tissues, which surround endothelial tubes.<sup>3,5</sup> The exception to this is in the central nervous system, where blood vessels recruit to their outer layer via the migration of neuroectodermal-derived mature mural cells, as typified by the development of the postnatal retinal vasculature.<sup>2,5</sup>

Consequences of failed mural cell recruitment range widely, depending on the degree of mural cell coverage. Midgestation lethality is seen in Alk5 knockout mice coinci-

Original received October 27, 2011; revision received June 11, 2012; accepted June 18, 2012. In May 2012, the average time from submission to first decision for all original research papers submitted to *Circulation Research* was 12.0 days.

From the Molecular Medicine Unit, UCL Institute of Child Health, UCL, London, United Kingdom (A.R., K.N.D.); the Department of Physiology, Anatomy, and Genetics, University of Oxford, Oxford, United Kingdom (N.S., P.R.R.); and Laboratory of Lymphocyte Signalling and Development, The Babraham Institute, Cambridge, United Kingdom (M.T.).

\*These authors contributed equally to this work.

The online-only Data Supplement is available with this article at <http://circres.ahajournals.org/lookup/suppl/doi:10.1161/CIRCRESAHA.111.259846/-/DC1>.

Correspondence to Paul R. Riley, PhD, Department of Physiology, Anatomy and Genetics, University of Oxford, South Parks Road, Oxford, OX1 3PT, UK. E-mail [paul.riley@dpag.ox.ac.uk](mailto:paul.riley@dpag.ox.ac.uk)

© 2012 American Heart Association, Inc.

*Circulation Research* is available at <http://circres.ahajournals.org>

DOI: 10.1161/CIRCRESAHA.111.259846

**Non-standard Abbreviations and Acronyms**

<b>HUVECs</b>	human umbilical vein endothelial cells
<b>PAI-1</b>	plasminogen activator inhibitor-1
<b>PDGF-B</b>	platelet-derived growth factor-B
<b>qRT-PCR</b>	quantitative reverse transcription polymerase chain reaction
<b>shRNA</b>	short hairpin RNA
<b>SM<math>\alpha</math>A</b>	smooth muscle alpha-actin
<b>SM22<math>\alpha</math></b>	smooth muscle 22 alpha
<b>SM-MHC</b>	smooth muscle myosin heavy chain
<b>SRE</b>	<i>Smad</i> -responsive element
<b>T<math>\beta</math>4</b>	thymosin beta 4
<b>TGF<math>\beta</math></b>	transforming growth factor-beta
<b>VE-cadherin</b>	vascular endothelial cadherin
<b>VSMC</b>	vascular smooth muscle cell

dent with a failure to differentiate mural cells.<sup>6</sup> However, mutants with a partial loss of mural cells can survive to later stages. The PDGF receptor- $\beta$ -null mouse dies perinatally, probably due to hemorrhage and edema as a result of lack of structural support to blood vessels.<sup>7</sup> In contrast, the endothe-

lial-specific PDGF-BB knockout mouse survives into adulthood with reduced mural cell coverage but has deficiencies in renal and cardiac function.<sup>8</sup> Nevertheless, in all of these described mutants, some degree of mural cell contribution to blood vessels is still observed, indicating that additional signals are required for mural cell differentiation from progenitor cells.

Thymosin  $\beta$ 4 (T $\beta$ 4) is a 43-amino acid peptide encoded by the gene *Tmsb4x* on the X chromosome in mouse. It was initially identified as a G-actin-binding protein with the ability to regulate the cellular availability of actin monomers for the formation of polymeric F-actin.<sup>7</sup> In recent times, however, novel functions have been ascribed to T $\beta$ 4, based on its ability to affect cell behavior when applied extracellularly or in a paracrine fashion.<sup>7</sup> Notably, T $\beta$ 4 has been shown to improve cardiac function after ischemic injury.<sup>8-10</sup> These cardioprotective effects may be due in part to the ability of T $\beta$ 4 to stimulate the differentiation of new coronary vascular cells, including coronary VSMCs, and consequently facilitate the process of neovascularization within the infarcted myocardium.<sup>9</sup>

Although several groups have shown that exogenous T $\beta$ 4 can promote angiogenesis both in vitro and ex vivo,<sup>11,12</sup> the role T $\beta$ 4 plays in the systemic vasculature in vivo is unknown. We describe a requirement for endothelial T $\beta$ 4 in the

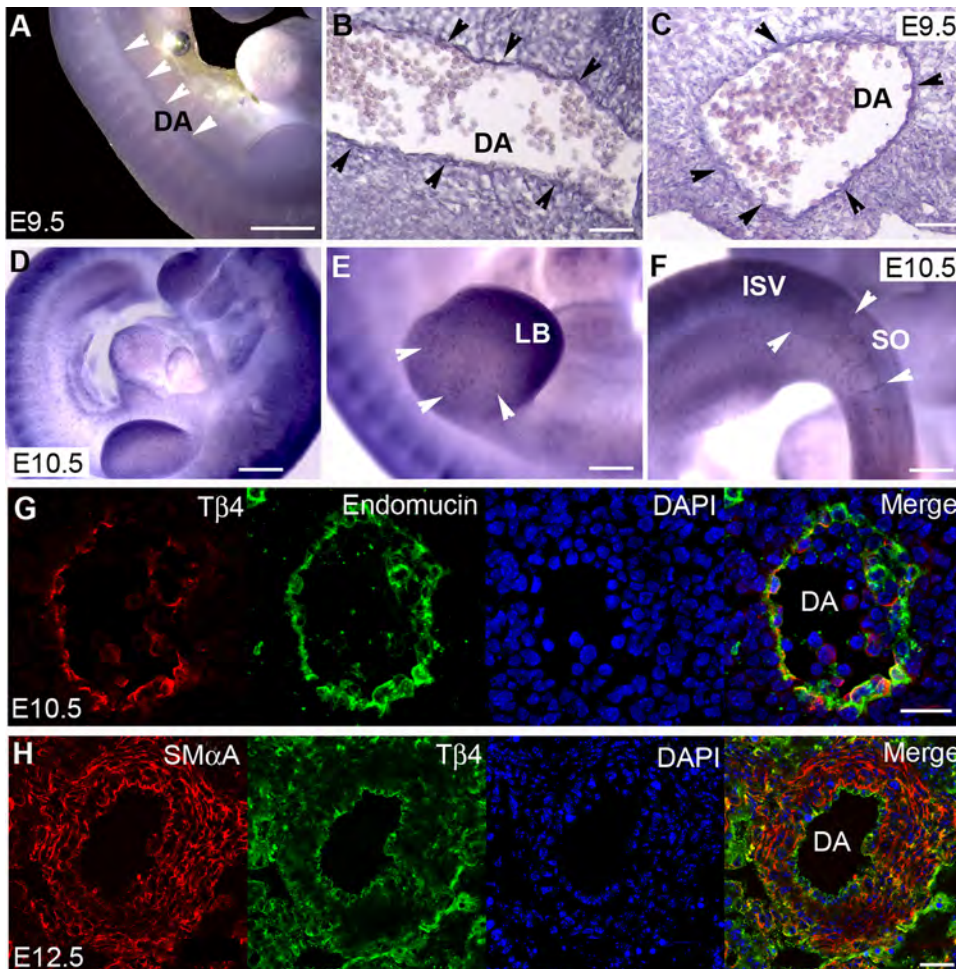


**Figure 1. T $\beta$ 4 is expressed in the endothelium of the developing aorta.** Whole-mount in situ hybridization at E9.5 reveals T $\beta$ 4 staining in the dorsal aorta (A, white arrowheads). Sagittal (B) and coronal (C) sections at E9.5 confirm the aortic expression of T $\beta$ 4 (black arrowheads highlight wall of dorsal aorta) (B and C). From E10.5, T $\beta$ 4 begins to be expressed in the microvasculature (D), notably highlighted by expression in the dermal vascular plexus of the limb bud (E) and the intersomitic vessels (F, white arrowheads). Expression of T $\beta$ 4 in the developing aorta colocalizes with the endothelial marker endomucin (G) at E10.5, whereas at E12.5 expression was also observed at a relatively lower level in the SM $\alpha$ A+ compartment (H). DA indicates dorsal aorta; ISV, intersomitic vessel; LB, limb bud. Scale bars: A, 500  $\mu$ m; B and C, 50  $\mu$ m; D, 400  $\mu$ m; E and F, 200  $\mu$ m; G, 20  $\mu$ m; H, 100  $\mu$ m.

**Table 1. A Significant Number of T $\beta$ 4-Null and Proportion of Endothelial-Specific T $\beta$ 4-Knockdown Embryos Die In Utero**

Genotype	Expected	E10.5	E14.5	P1
Global T $\beta$ 4 knockout				
+/-	25%	19 (21%)	73 (35%)	111 (33%)
-/-	25%	28 (31%)	40 (19%)	64 (19%)
+/ <i>Y</i>	25%	23 (26%)	60 (29%)	105 (31%)
-/ <i>Y</i>	25%	19 (21%)	34 (16%)	59 (17%)
Total		89	207	339
$\chi^2$		2.461	18.797	25.873
<i>P</i> value		0.482	3.01E-04	1.01E-05
Endothelial-specific T $\beta$ 4 knockdown				
Tie2+/+; HPRT+/+	25%	16 (25%)	22 (25%)	33 (32%)
Tie2Cre/+; HPRT+/+	25%	16 (25%)	24 (28%)	26 (25%)
Tie2+/+; T $\beta$ 4floxshRNA+/-	25%	23 (22%)	23 (27%)	25 (25%)
Tie2Cre/+; T $\beta$ 4floxshRNA+/-	25%	18 (28%)	17 (20%)	18 (18%)
Total		64	86	102
$\chi^2$		0.500	1.349	6.978
<i>P</i> value		0.919	0.718	0.073

Crossing of T $\beta$ 4 -/*Y* adult male mice with T $\beta$ 4 +/- adult females should result in equal proportions of T $\beta$ 4 +/*Y*, T $\beta$ 4 -/*Y*, T $\beta$ 4 +/-, and T $\beta$ 4 -/- in the F1. At E10.5, mendelian ratios are retained, however, by E14.5 and between E14.5 and birth (postnatal day 1), embryonic lethality has caused a significant number ( $P=3.01 \times 10^{-4}$  and  $P=1.1 \times 10^{-5}$ , respectively) of T $\beta$ 4 -/*Y* and T $\beta$ 4 -/- to die in utero. Endothelial-specific knockdown of T $\beta$ 4 by intercrossing Tie2-Cre/+ and HPRT-targeted T $\beta$ 4floxshRNA+/- results in a loss of knockdown embryos between the equivalent stages of E10.5 and 14.5 ( $P=0.718$ ) and E14.5 and P1 ( $P=0.073$ ), approaching statistical significance by P1. Embryonic lethality in both models is attributed to systemic vascular hemorrhaging (E10.5 to E14.5) and coronary vessel defects (E14.5 to P1).

differentiation of mesoderm-derived mural cells to contribute to the stability of the developing vasculature: a function mediated through synergy with the TGF $\beta$  pathway.

## Methods

An expanded Methods section is available in the Online Data Supplement.

### Mouse Lines

Mice were housed and maintained in a controlled environment, and all procedures were performed in accordance with the Animals (Scientific Procedures) Act 1986, (Home Office, United Kingdom). Global T $\beta$ 4 KO mice were generated by deleting exon 2 of the *Tmsb4x* locus and maintained on a C57Bl6/J background for more than 20 generations. Endothelial-specific T $\beta$ 4 knockdown mice were generated by crossing female mice, containing a previously described T $\beta$ 4 short hairpin RNA (shRNA)<sup>9</sup> targeted to the hypoxanthine phosphoribosyltransferase locus with Tie2-Cre male mice.<sup>13</sup> A cardiac-specific T $\beta$ 4 shRNA knockdown strain has been previously described,<sup>10</sup> using a Nkx2-5-Cre knock-in<sup>14</sup> crossed with the T $\beta$ 4 shRNA knockdown strain.

### Histology, Immunofluorescence, and In Situ Hybridization

Standard histological, immunohistochemical, immunofluorescence, and in situ hybridization were performed on frozen or paraffin embryo sections or on whole-mount fixed embryos or retinas harvested at postnatal day 6, as described in full in the Online Supplement.

### Real-Time PCR

Real-time quantitative PCR (qRT-PCR) was performed according to a standard  $\Delta\Delta$ CT protocol using SYBR green (Applied Biosystems). Primer sequences are given in the Online Supplement.

### Cell Culture

10T1/2 cells and A404 cells were maintained under standard conditions. For stimulation experiments, cells were treated for 4 days with PBS vehicle control, 1  $\mu$ g/mL T $\beta$ 4, 2 ng/mL TGF $\beta$ , or 1  $\mu$ g/mL T $\beta$ 4 plus 2 ng/mL TGF $\beta$  before RNA extraction using Trizol reagent (Invitrogen). For Smad 2 phosphorylation assays, A404 cells were serum-starved (0.5% fetal calf serum) overnight before stimulation, as above, for 20 minutes before protein extraction and standard Western blotting. For coculture experiments, early-passage human umbilical vein endothelial cells (HUVECs) were cultured in 50:50 A404:HUVEC medium (endothelial cell growth medium, PromoCell) for 24 hours; cells were counted, and an equal number of A404 cells were plated in each well. Thereafter, cells were cocultured in A404 medium for 4 days, with or without the addition of a neutralizing rabbit polyclonal anti-T $\beta$ 4 antibody (1:250; Immundiagnostik). 10T1/2 cells were transfected with Smad activity luciferase reporter plasmids (SA Biosciences) using Effectene transfection reagent (Qiagen) according to the manufacturer's instructions. After 16 hours, cells were serum-starved overnight (0.5% FCS in DMEM+Glutamax) before stimulation for 6 hours in the presence of 100 ng/mL T $\beta$ 4, 2 ng/mL TGF $\beta$ , 100 ng/mL T $\beta$ 4 plus 2 ng/mL TGF $\beta$ , or a PBS vehicle control. Smad activity-dependent firefly luciferase activity was measured by dual luciferase reporter assay (Promega).

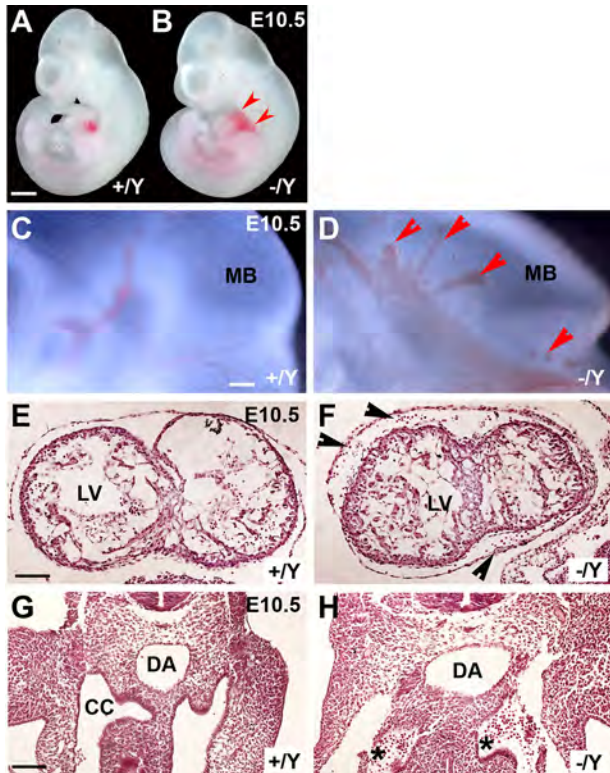


**Figure 2. Embryos lacking  $T\beta 4$  reveal a gross hemorrhagic phenotype.** A proportion of E10.5  $T\beta 4$   $-/Y$  embryos displayed overt pericardial hemorrhage (A and B, red arrowheads) and cranial hemorrhage in the midbrain region (C and D, red arrowheads). Bleeding into the pericardium was confirmed by sagittal section through  $T\beta 4$   $+/Y$  and  $-/Y$  hearts at E10.5 (E and F, black arrowheads highlight presence of blood in pericardial cavity). Coelomic cavity hemorrhage was also seen in the  $T\beta 4$   $-/Y$  embryos (G and H; black asterisks indicate coelomic bleeding). CC indicates coelomic cavity; DA, dorsal aorta; LV, left ventricle; MB, midbrain. Scale bars: A as applies to B, 500  $\mu\text{m}$ ; C as applies to D, 50  $\mu\text{m}$ ; E as applies to F, 50  $\mu\text{m}$ ; G as applies to H, 100  $\mu\text{m}$ .

### Exon Array Analysis

Micro-arrays were performed on Affymetrix Mouse Exon 1.0ST arrays. Raw data were processed with Affymetrix expression console software before being analyzed for gene expression changes in Partek. Statistics were performed in R and pathway analysis performed using the Metacore software (Genego).

### Statistics

Statistical analysis was performed with Graphpad Prism software. Contingency tables were analyzed by  $\chi^2$  test. Two-tailed, unpaired, nonparametric  $t$  tests were used for all other statistical tests.

## Results

### $T\beta 4$ Is Expressed in the Endothelium of the Developing Embryo

To investigate vascular expression of  $T\beta 4$  during development, whole-mount and section in situ hybridization was performed on midgestation embryos.  $T\beta 4$  was expressed in the dorsal aorta of the developing embryo from E9.5 onward (Figure 1A, 1B, and 1C). At E10.5,  $T\beta 4$  expression appeared relatively ubiquitous at low resolution (Figure 1D) but was

detected in all developing blood vessels in the embryo (Figure 1D through 1F), including those within the developing limb bud (Figure 1E) and the intersomitic vessels (Figure 1F). Immunofluorescence analysis revealed that  $T\beta 4$  was predominantly expressed in the developing endothelium at E10.5, which was retained at E12.5. Relatively weaker expression was observed in the mural cell population of the dorsal aorta at E12.5, consistent with the onset of a more differentiated smooth muscle cell layer (Figure 1G and 1H).

### Loss of $T\beta 4$ Causes Hemorrhage Due to a Defect in Mural Cell Recruitment to Developing Vessels

To determine whether  $T\beta 4$  plays an essential role during the development of the systemic vasculature, a global loss of function model of  $T\beta 4$  was created by replacing exon 2 of the *Tmsb4x* gene with a neomycin resistance cassette resulting in a functionally null allele (Online Figure I). Hemizygous null male ( $T\beta 4$   $-/Y$ ) mice reach adulthood, but in reduced numbers, indicating a degree of embryonic lethality (Table 1). The loss of  $T\beta 4$   $-/Y$  embryos was progressive from insignificant lethality before and up to E10.5 (21% versus 25% expected;  $P=0.482$ ) through to significantly reduced recovery of mutants at E14.5 (16% versus 25% expected;  $P=3.01 \times 10^{-4}$ ) and up to birth (17% versus 25% expected;  $P=1.01 \times 10^{-5}$ ), indicating incomplete penetrance (Table 1). When E10.5  $T\beta 4$   $-/Y$  embryos were examined, it was apparent that approximately 10% of  $T\beta 4$   $-/Y$  embryos displayed abnormal accumulation of blood in their hearts (Figure 2A and 2B). Mutant embryos also revealed extensive cranial bleeding in the midbrain region compared with  $+/Y$  controls (Figure 2C and 2D) and in axial sections there was clear evidence of both pericardial and coelomic cavity hemorrhage (Figure 2E through 2H). Severe vascular hemorrhaging at E10.5 was incompatible with continued survival accounting for the significant loss of  $T\beta 4$   $-/Y$  mutant between E10.5 and E14.5 (Table 1). Over the course of the studies, we observed a reduction in embryonic lethality, reflecting an overall increase from approximately 60% to 80% survival of  $T\beta 4$   $-/Y$  mutant mice to postnatal stages. This was coincident with a reduced incidence of the more severe hemorrhagic phenotype identified at E10.5, down from 44% to 20%, and reflected in an increased recovery of viable embryos at E14.5. The data in Table 1 represent current embryonic lethality versus survival rates against expected mendelian ratios.

Such hemorrhagic phenotypes can arise through defective mural cell investiture of developing blood vessels.<sup>15,16</sup> Thus,  $T\beta 4$   $-/Y$  embryos were examined for mural cell defects. Immunofluorescence studies for NG2, a marker that we initially confirmed as specific for mural cells and excluded from the developing endothelium (Figure 3A and 3B), showed that by E10.5 wild-type embryos displayed a dorsal aorta invested with NG2-positive mural cells (Figure 3C). This mural cell coverage was significantly reduced in  $T\beta 4$   $-/Y$  embryos (consistent with the hemorrhagic phenotype observed in Figure 2H) in comparison to littermate  $T\beta 4$   $+/Y$  controls (Figure 3C through 3F). The mural cell coverage directly correlated with severity of phenotype, observed in

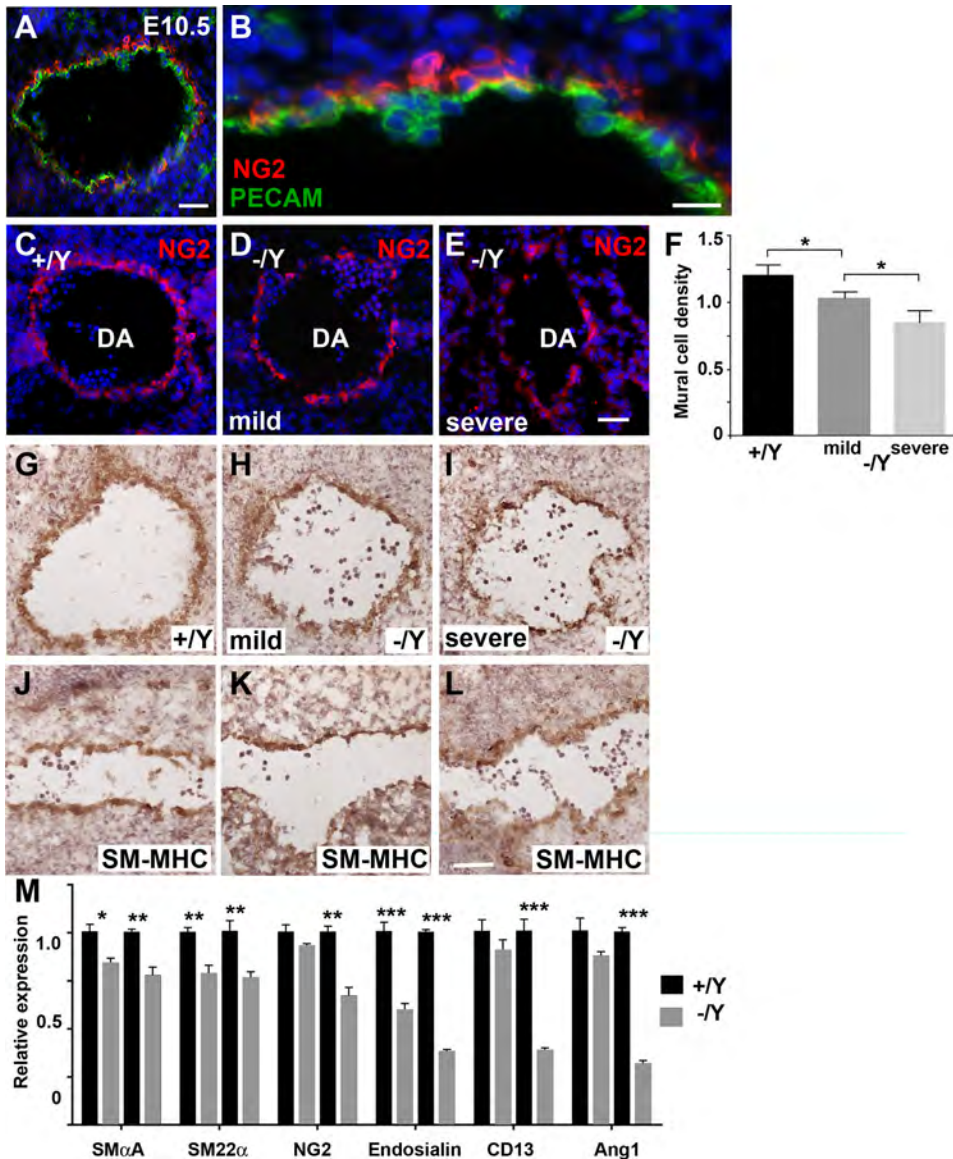


**Figure 3. Impaired mural cell coverage in  $T\beta 4$ -null vasculature.** Immunofluorescence staining for the mural cell-specific marker NG2, which is excluded from the PECAM positive endothelium (A and B), revealed that by E10.5  $T\beta 4$   $-/Y$  embryos which exhibited a mild phenotype with intact vasculature (mild) and  $T\beta 4$   $-/Y$  mutants with hemorrhaging (severe) display reduced coverage of mural cells in comparison to control  $T\beta 4$   $+/Y$  embryos (C through E). This defect in mural cell investiture is quantifiable and statistically significant (F;  $n=6$  embryos per genotype;  $*P\leq 0.05$ ). Reduced mural cell coverage was confirmed by immunohistochemistry for smooth muscle myosin heavy chain (SM-MHC) in the wall of the aorta in  $T\beta 4$   $+/Y$  (G and J) and  $-/Y$  mild (H and K) and severely affected (I and L) littermates, which revealed reduced and irregular staining of the mutant vessel wall in both transverse and sagittal sections through the aorta. qRT-PCR studies reveal significant global defects in the expression of a large panel of mural cell marker genes between somite matched pairs of E10.5  $T\beta 4$   $+/Y$  and  $T\beta 4$   $-/Y$  embryos implying a reduction in mural cells across mutant embryos ( $n=5$  embryo pairs run in triplicate per qRT-PCR run) (M). Ang1 indicates angiopoietin 1; DA, dorsal aorta. Scale bars: A, 30  $\mu\text{m}$ ; B, 20  $\mu\text{m}$ ; E as applies to C and D, 20  $\mu\text{m}$ ; L as applies to G through L, 30  $\mu\text{m}$ . Statistics:  $*P\leq 0.05$ ,  $**P\leq 0.01$ ,  $***P\leq 0.001$ ; 2-tailed Mann-Whitney  $U$  test.

and D, 20  $\mu\text{m}$ ; L as applies to G through L, 30  $\mu\text{m}$ . Statistics:  $*P\leq 0.05$ ,  $**P\leq 0.01$ ,  $***P\leq 0.001$ ; 2-tailed Mann-Whitney  $U$  test. Error bars represent standard error of the mean.

$T\beta 4$   $-/Y$  embryos, such that investiture was less significantly reduced in mildly affected embryos, in which the vascular wall appeared intact, as compared with severely affected mutants with evident hemorrhaging (Figure 3F). A reduced mural cell pool, impaired support of the mutant  $-/Y$  dorsal aorta, and correlation with severity of phenotype was further illustrated by immunohistochemistry for smooth muscle myosin heavy chain (SM-MHC) in transverse and sagittal sections Figure 3G through 3L). Globally impaired mural cell development in E10.5  $T\beta 4$   $-/Y$  embryos was confirmed by downregulation of a wide panel of mural cell markers in somite matched pairs of E10.5  $T\beta 4$   $+/Y$  and  $T\beta 4$   $-/Y$  embryos, quantified by qRT-PCR. Significant changes in gene expression were observed for markers of VSMCs such as smooth muscle  $\alpha$ -actin (SM $\alpha$ A) and smooth muscle 22 $\alpha$  (SM22 $\alpha$  as well as pericyte markers such as endosialin, NG2, CD13, and angiopoietin 1 (Figure 3M). Consistent with the ubiquitous expression of  $T\beta 4$  in developing blood vessels,

$T\beta 4$   $-/Y$  embryos at E14.5, displayed statistically significant levels of dermal hemorrhage compared with littermate controls (Online Figure IIA through C). Immunostaining of the skin from E14.5  $T\beta 4$   $-/Y$  embryos for SM $\alpha$ A demonstrated a qualitative lack of mural cell-derivatives in comparison to specimens from control  $T\beta 4$   $+/Y$  littermates (Online Figure IID and E). We next examined the integrity of the developing endothelium in  $T\beta 4$   $+/Y$  versus  $T\beta 4$   $-/Y$  aortas (Figure 4A and 4B). Even in selected areas of the walls of the dorsal aortas which appeared to have a disrupted endothelium by gross histological staining (Figure 4A and 4B; black inset boxes), immunofluorescence for the endothelial-specific adhesion molecule, VE-cadherin (Figure 4C and 4D), suggested that the endothelial cell contacts were intact across all genotypes, including both in mildly and severely affected mutants relative to  $T\beta 4$   $+/Y$  controls (Figure 4E through 4G). This was supported by immunostaining for zona occludens 1 (ZO-1) (Figure 4H through 4N), a marker of

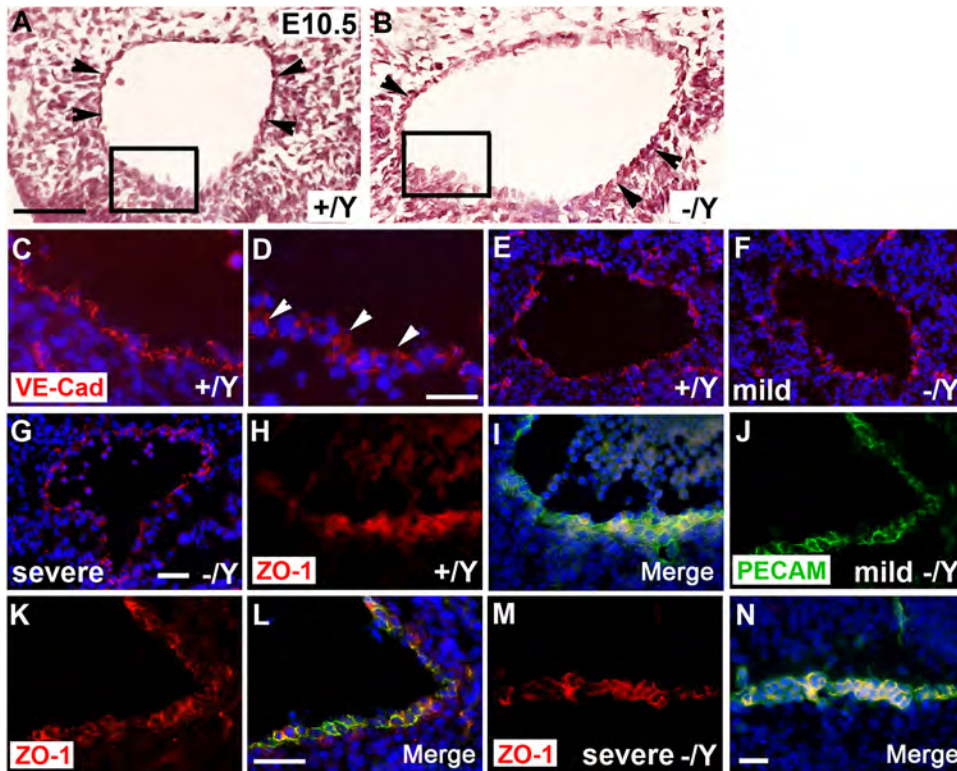


**Figure 4. Endothelial integrity is maintained in dorsal aortas of  $T\beta 4$ -null embryos at E10.5.** Histological (hematoxylin and eosin-stained) sections through the dorsal aorta of  $T\beta 4$   $+/Y$  and  $-/Y$  littermate embryos at E10.5 reveal the mutant aorta to be expanded in diameter and the vessel wall to be irregular (**A** and **B**). Black boxes in **A** and **B** depict selected areas of vessel wall in both  $T\beta 4$   $+/Y$  and  $-/Y$  aortas for which the endothelium appears irregular although intact as represented in **C** and **D**, respectively; black arrowheads in **B** highlight grossly intact endothelium. Immunostaining for the endothelial adhesion marker VE-cadherin reveals that endothelial contact is maintained in the mutant  $T\beta 4$   $-/Y$  vessel lumen comparable to that observed in the  $T\beta 4$   $+/Y$  controls (**C** and **D**); white arrowheads in **D** highlight endothelial cell contact, further evident by comparing the endothelium of a  $+/Y$  control aorta (**E**) with that of a mild (**F**) and severe (**G**) mutant. The

integrity of the endothelium after loss of  $T\beta 4$  was confirmed by positive immunostaining for the tight junction marker ZO-1, between  $+/Y$  (**H** and **I**), mildly affected (**J** through **L**), and severely affected (**M** and **N**) mutant littermates. Scale bars: **A** as applies to **B**, 100  $\mu\text{m}$ ; **D** as applies to **C**, 40  $\mu\text{m}$ ; **G** as applies to **E** through **G**, 20  $\mu\text{m}$ ; **L** as applies to **J** through **L**, 20  $\mu\text{m}$ ; **N** as applies to **M**, 20  $\mu\text{m}$ .

endothelial tight junctions, which revealed an integral endothelium within  $T\beta 4$   $-/Y$  aortas (Figure 4J through 4N) comparable to that of littermate controls (Figure 4H and 4I).

To confirm that the mural cell defects observed in  $T\beta 4$   $-/Y$  embryos were due to a deficiency of  $T\beta 4$  in the endothelium, as suggested by the expression data (Figure 1), rather than a lack of  $T\beta 4$  acting cell autonomously in mural cells, we made use of a mouse strain that enables transcription of a  $T\beta 4$  shRNA under the control of Cre recombinase with the potential for tissue-specific knockdown of  $T\beta 4$ .<sup>9</sup> By crossing this mouse with a Tie2-Cre strain,<sup>13</sup> knockdown of  $T\beta 4$  specifically in the developing endothelium was achieved (Figure 5). Initially, we observed a gross hemorrhagic phenotype (including cranial, pericardial, and coelomic cavity bleeding) in 30% of the endothelial-specific  $T\beta 4$ -knockdown embryos at E10.5 ( $n=24$  embryos analyzed), which was equivalent to the one-third documented for the global  $T\beta 4$   $-/Y$  mutants. In addition, we recorded an overall incidence of embryonic lethality in Tie2-Cre  $T\beta 4$  shRNA animals of 12% (animals lost in utero between E10.5 and E14.5 and up to P1 according to expected mendelian ratios at birth) compared with 17% for the  $-/Y$  knockout animals (Table 1). The reduced incidence of loss in utero in the EC specific  $T\beta 4$ -shRNA model may reflect both inefficient knockdown via the Cre/shRNA as demonstrated by qRT-PCR (Figure 5) and additional developmental roles for  $T\beta 4$  highlighted by global loss of function, such as an essential requirement in epicardial-derived coronary vasculogenesis.<sup>9</sup> The latter was confirmed as a contributory factor to the differential embry-

onic lethality between E14.5 and P1 by analyzing the coronary vasculature of  $T\beta 4$   $-/Y$  embryos at E14.5 (Online Figure III). We observed a significant incidence of VSMCs abnormally residing within the epicardial layer and reduced presence in the underlying myocardium, compared with  $T\beta 4$   $+/Y$  littermate controls (Online Figure IIIA and B), a phenotype consistent with that described after myocardial shRNA knockdown of  $T\beta 4$ .<sup>9</sup>

Serial sections through the developing dorsal aorta of Tie2-Cre  $T\beta 4$  shRNA embryos revealed defective NG2-positive mural cell recruitment to the vessel wall in comparison to Cre-only littermate controls (Figure 5A and 5B). The defective recruitment was equivalent to that observed after global knockdown of  $T\beta 4$  (Figure 3C through 3E). Knockdown of  $T\beta 4$  expression in Tie2-Cre  $T\beta 4$  shRNA embryos was confirmed by qRT-PCR on isolated dorsal aortas (Figure 5C) and protein knockdown via immunostaining for  $T\beta 4$  with Image J quantification (Online Figure IV); abrogation of  $T\beta 4$  mRNA and protein expression was incomplete at approximately 40% of control levels in each case (Figure, 5C; Online Figure IV). Mural cell density around the wall of the aorta was quantitatively assessed by cell counts across serial sections, which revealed a significant reduction in mural cell coverage after endothelial-specific knockdown of  $T\beta 4$  (Figure 5D). Finally, as for the global knockout model, we assessed VE-cadherin expression by immunofluorescence to reveal that the endothelium was intact in Tie2-Cre  $T\beta 4$  shRNA aortas (Figure 5E and 5F). Collectively, these data reveal a non-cell autonomous role for endothelial  $T\beta 4$  in

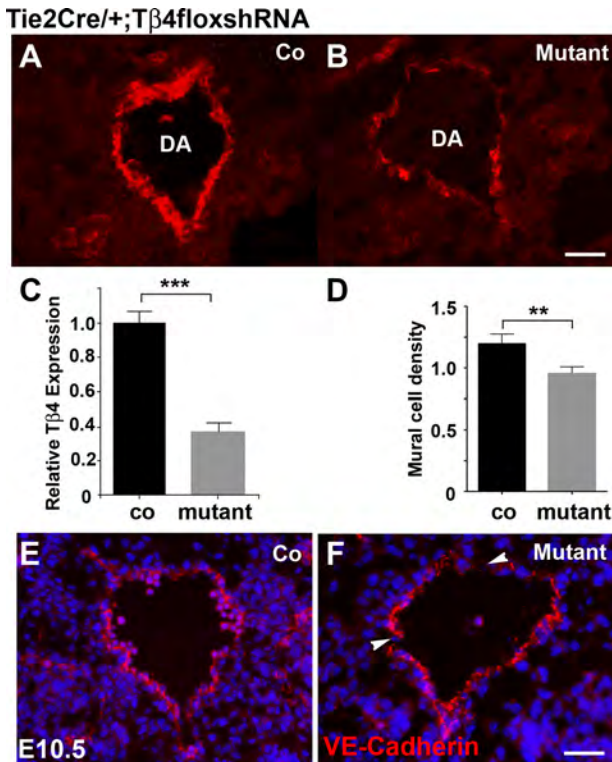


**Figure 5. Impaired mural cell coverage in endothelial-specific  $T\beta 4$ -knockdown vasculature.** Mutant Tie2-Cre- $T\beta 4$ shRNA embryos at E10.5, revealed a deficit in NG2-positive mural cells in comparison to control littermates expressing Cre alone (**A** and **B**). Significant knockdown of  $T\beta 4$  was confirmed by qRT-PCR on dissected aortas from E10.5 control and mutant embryos (**C**). The defect in mural cell coverage in the knock-down vasculature was both quantifiable and highly significant (**D**;  $n=6$  per genotype;  $P\leq 0.01$ ). Immunostaining for VE-cadherin confirmed the endothelium was intact in the mutant dorsal aorta after endothelial-specific knockdown of  $T\beta 4$  (**E** and **F**; white arrowheads highlight endothelial cell contacts). Scale bars: **B** as applies to **A**,  $20\ \mu\text{m}$ ; **F** as applies to **E**,  $30\ \mu\text{m}$ ; Statistics:  $**P\leq 0.01$ ,  $***P\leq 0.001$ ; 2-tailed Mann-Whitney  $U$  test. Error bars represent standard error of the mean.

determining mural cell/VSMC coverage of the systemic vasculature during development.

### Endothelial $T\beta 4$ Stimulates Differentiation of Mesodermal Cells to a Mature Mural Cell Phenotype

Mural cell defects in developmental mutants have previously been attributed to either aberrant migration, survival, proliferation, or differentiation of mural cells.<sup>2</sup> The postnatal retinal vasculature, consistent with its status as a central nervous system tissue, derives a mural cell layer via the migration of phenotypically mature mural cells along the developing vascular plexus. Whereas  $T\beta 4$  is expressed in the primary plexus vasculature of the early postnatal (P6) retina (Online Figure VA and B), P6 retinas from  $T\beta 4$   $-/Y$  mice did not show any defect in mural cell coverage when compared with  $T\beta 4$   $+/Y$  littermate controls (Online Figure VC through E), suggesting that impaired migration of mural cells is unlikely to be responsible for the defective mural cell

coverage of  $T\beta 4$   $-/Y$  embryos. In addition, mural cells displayed no overtly abnormal levels of proliferation or apoptosis, as measured by phospho-histone H3 or cleaved caspase 3 immunofluorescence staining, respectively, in either  $T\beta 4$   $+/Y$  or  $T\beta 4$   $-/Y$  embryos (Online Figure VIA through F), thus ruling out the possibility that the mural cell defects observed were due to defective mural cell hyperplasia or survival.

Blood vessels in mesoderm-derived tissues are thought to recruit mural cells via the in situ differentiation of mesoderm progenitors into mature mural cells.<sup>5</sup> Given that mural cell defects in  $T\beta 4$   $-/Y$  embryos are present only in mesodermal tissues, such as the aorta and subdermal vessels and not in tissues that derive their mural cells via migration, such as the postnatal retina, we investigated whether  $T\beta 4$  acts to induce mesoderm differentiation into a mature mural cell lineage. Initially, we assessed the ability of exogenous  $T\beta 4$  to stimulate the differentiation of a P19 embryonal carcinoma cell line known as A404,<sup>17</sup> clonally selected for a propensity to differentiate into mural cells. Treatment of A404 mural cell progenitor cells with synthetic  $T\beta 4$  resulted in an increased number of SM22 $\alpha$ - and SM $\alpha$ A-positive cells in culture compared with vehicle-treated controls (Figure 6A, 6B, 6E, and 6F). TGF $\beta$  was used as a positive control in these experiments and resulted in an equivalent increase in the incidence of SM22 $\alpha$ - and SM $\alpha$ A-positive cells that was further augmented by the combined addition of both  $T\beta 4$  and TGF $\beta$  (Figure 6C, 6D, 6G, and 6H). The phenotypic changes in the A404 cells and coincident expression of the smooth muscle differentiation markers in culture were accompanied by a significant upregulation of mural gene expression, as quantified by qRT-PCR. Markers of both VSMCs such as SM $\alpha$ A and SM22 $\alpha$  and pericytes, such as endosialin and desmin, were all significantly upregulated (Figure 6I). These data indicate that  $T\beta 4$  can act in a paracrine fashion to stimulate mural cell differentiation from mesoderm.

### $T\beta 4$ Stimulates Mural Cell Differentiation by Enhancing the Activity of TGF $\beta$ Signaling

To gain greater insight into the molecular mechanisms underlying the role of  $T\beta 4$  in mural cell differentiation, gene expression arrays were carried out on E12.5  $T\beta 4$   $-/Y$  and  $+/Y$  embryos and compared with array data from  $T\beta 4$   $+/Y$  and  $-/Y$  adult hearts to further facilitate the identification of  $T\beta 4$ -dependent gene expression. Metacore software from GeneGo was used to highlight the expression changes of signaling factors in the embryo and adult heart datasets and identify the most likely underlying pathways. Four of the top 5 highlighted pathways included TGF $\beta$  (Table 2), previously highlighted as a key molecule involved in mural cell differentiation.<sup>17,18</sup> Thus, we hypothesized that  $T\beta 4$  may exert its effects on mural cell differentiation by interaction with and/or modulation of the TGF $\beta$  pathway.

Activation of the canonical TGF $\beta$  pathway in mural cells leads to the transcription of stereotypical TGF $\beta$ -responsive genes such as plasminogen activator inhibitor-1 (PAI-1), Id-1, and c-myc.<sup>19,20</sup> Levels of the mRNAs encoding these proteins can be used as a read-out of TGF $\beta$  pathway activity.

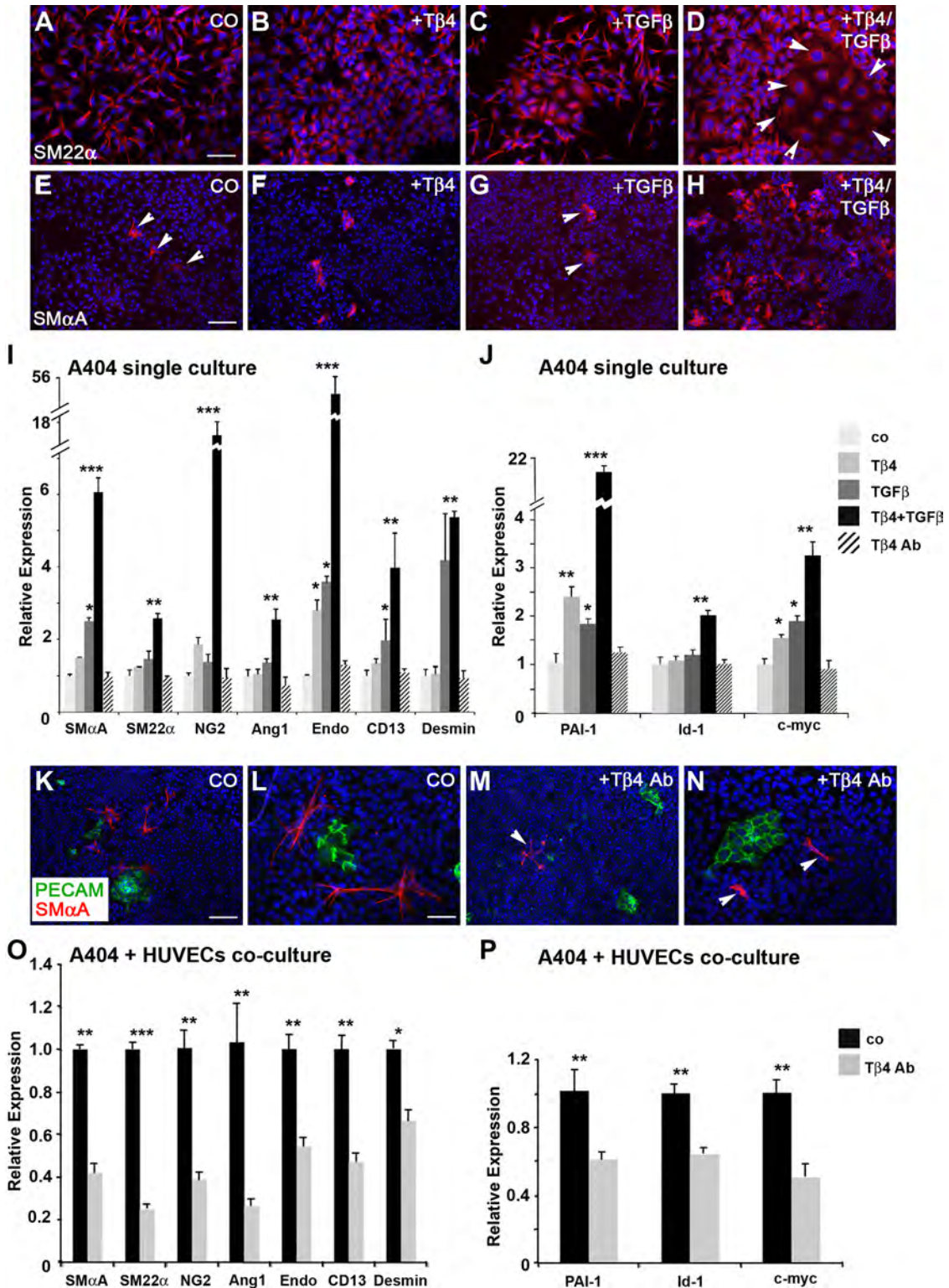


**Figure 6. Tβ4 induces in vitro mural cell differentiation via the TGFβ signaling pathway.** Culture of A404 cells in the presence of exogenous Tβ4 led to an upregulation in the smooth muscle cell markers, SM22α and SMαA, and corresponding change in A404 progenitor morphology (A, B, E, and F; white arrowheads in E highlight background differentiation in control cultures). Ectopic administration of TGFβ served as a positive control for mural cell differentiation (C and G; white arrowheads in G highlight TGFβ-induced differentiation), which in combination with Tβ4 augmented a further significant effect on cell morphology and smooth muscle cell marker expression (D and H; white arrowheads in D highlight differentiated cells). The addition of Tβ4 alone or in combination with TGFβ resulted in a significant upregulation of a wide panel of mural cell markers as measured by qRT-PCR (I; n=8 per treatment group) and also significantly enhanced the expression of the TGFβ target genes PAI-1, Id-1, and c-myc, an effect that was blocked by the addition of Tβ4-neutralizing antibody (J). Coculture of A404 cells with HUVECs (PECAM+) induced differentiation of the progenitors as indicated by a change in cell morphology and expression of SMαA (K and L). A404 differentiation was inhibited by the addition of Tβ4-neutralizing antibody (M and N), suggesting that Tβ4 is a key paracrine factor secreted from HUVECs to regulate mural cell differentiation. HUVEC

**Table 2. Metacore Analyses of Array Data Revealed Misregulation of the TGF $\beta$  Pathway in the T $\beta$ 4-Null Background**

Rank	Gene	NCBI Accession	Fold Change	Heart or Embryo	Description
1	Actb	NM_007393	-8.6	H	Actin B
	Pfn1	NM_011072	-10.8	H	Profilin1
	Robo4	NM_028783	-6.5	E	Roundabout homologue 4
	TGF $\beta$ 1	NM_011577	-8.8	H	TGF $\beta$ 1
	Rac1	NM_009007	+6.8	E	Ras-related C3 botulinum toxin substrate 1
2	Gas8	NM_018855	+6.9	E	Growth arrest specific 8
	TGF $\beta$ 1	NM_011577	-8.8	H	TGF $\beta$ 1
	Trp53	NM_011640	-8.6	H	Transformation-related protein 53
	Nme2	NM_008705	-6.1	E	Nonmetastatic cells 2, protein
3	Anxa1	NM_010730	+9.3	H	Annexin A1
	Stx4a	NM_009294	+7.0	E	Syntaxin 4a
	Rac1	NM_009007	+6.8	E	Ras-related C3 botulinum toxin substrate 1
4	Jun-B	NM_008416	+6.0	H	Jun-B oncogene
	TGF $\beta$ 1	NM_011577	-8.8	H	TGF $\beta$ 1
	Adam12	NM_007400	-7.0	E	A disintegrin and metalloproteinase 12
5	Nes	NM_016701	+8.6	E	Nestin
	TGF $\beta$ 1	NM_011577	-8.8	H	TGF $\beta$ 1
	Rac1	NM_009007	+6.8	E	Ras-related C3 botulinum toxin substrate 1

The top 200 hundred upregulated and downregulated genes identified by affymetrix exon array between T $\beta$ 4 +/Y and T $\beta$ 4 -/Y E12.5 embryos and T $\beta$ 4 +/Y and T $\beta$ 4 -/Y adult hearts were analyzed using Genego Metacore software <http://www.genego.com/metacore.php>. Reverse pathway analysis based on altered gene expression levels and comparison to a systems biology database identified potential disrupted signaling pathways in the T $\beta$ 4 -/Y embryos. Four of the top 5 potentially disrupted pathways involved TGF $\beta$  as a major signaling node. Displayed are the nodes present in the top 5 ranked putative pathways alongside levels of differential expression per transcript in the exon arrays.

Treatment of A404 cells with T $\beta$ 4 led to significant upregulation of these TGF $\beta$  target genes, comparable to that induced by TGF $\beta$  alone, as measured by qRT-PCR, and, moreover, combined T $\beta$ 4 and TGF $\beta$  acted to further significantly increase expression of all 3 target genes, indicating that T $\beta$ 4 can enhance TGF $\beta$  signaling in these cells (Figure 6J). We next examined cocultures of A404 progenitors with HUVECs, plus or minus T $\beta$ 4 neutralizing antibody. Importantly, T $\beta$ 4 antibody alone had no effect on A404 differentiation per se as confirmed by addition to A404 cultures followed by qRT-PCR (Figure 6I and 6J; black hatched bars). HUVECs express T $\beta$ 4 at high levels,<sup>21</sup> and in the control setting, HUVEC coculture brought about differentiation of the A404 cells, as indicated by changes in cell morphology (adoption of a more elongated and differentiated phenotype) and expression of SM $\alpha$ A (Figure 6K and 6L). However, the addition of T $\beta$ 4 antibody significantly blocked the visible differentiation of A404 cells in culture (Figure 6M and 6N) and significantly reduced the expression of both mural cell markers (Figure 6O) and the TGF $\beta$  targets PAI-1, Id-1 and c-myc (Figure 6P).

Binding of TGF $\beta$  ligands to their cognate receptors leads to phosphorylation of Smad adaptor proteins.<sup>22</sup> Treatment of A404 cells with T $\beta$ 4 alone resulted in increased levels of

phospho-Smad2, to an equivalent level to TGF $\beta$  alone (Figure 7A). Most notably, T $\beta$ 4 in combination with TGF $\beta$  was able to induce higher levels of Smad2 phosphorylation than TGF $\beta$  treatment alone (Figure 7A). To investigate whether T $\beta$ 4 might be required for TGF $\beta$  signaling via Smad2 in vascular development, we assessed phospho-Smad2 levels in global T $\beta$ 4 -/Y embryos and observed a significant downregulation of phospho-Smad2 in both mildly and severely affected -/Y mutants compared with littermate (+/Y) controls (Figure 7B).

These data collectively suggest that endothelial T $\beta$ 4, acting in a paracrine fashion, regulates mural cell differentiation to VSMCs via synergistic activation of the TGF $\beta$  signaling pathway.

### Inhibition of the TGF $\beta$ Pathway Correlates With the Penetrance of Hemorrhage in T $\beta$ 4-Null Aortas and Alterations in Downstream Signaling

To further determine whether TGF $\beta$  signaling was impaired with loss of T $\beta$ 4 in vivo, we examined aortas at E10.5 from T $\beta$ 4-null mutants, with or without evidence of vascular

**Figure 6 (Continued).** coculture also upregulated the wide panel of mural cell markers as measured by qRT-PCR, which were downregulated in the presence of T $\beta$ 4-blocking antibody (O). An equivalent HUVEC dependent upregulation was observed for the TGF $\beta$  target genes in A404 cultures, which was also antagonized by T $\beta$ 4 antibody treatment (P). Scale bars: A as applies to A through D, 10  $\mu$ m; E as applies to E through H, 10  $\mu$ m; K as applies to M, 10  $\mu$ m; L as applies to N, 5  $\mu$ m. Statistics: \* $P$ ≤0.05, \*\* $P$ ≤0.01, \*\*\* $P$ ≤0.001; 2-tailed Mann-Whitney  $U$  test. Error bars represent standard error of the mean.

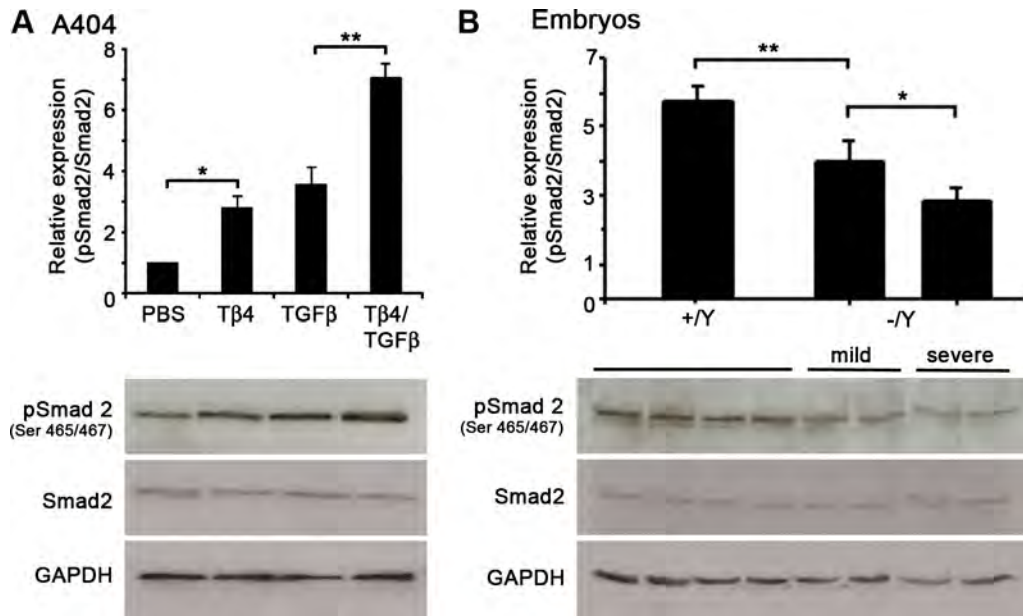


**Figure 7. Gain and loss of  $T\beta 4$  leads to an upregulation and downregulation of  $TGF\beta$  signaling, respectively, during in vitro and in vivo mural cell differentiation.** Levels of phosphorylated Smad 2 (pSmad2) (A), as determined by Western analyses and scanning densitometry, were increased in A404 cells cultured in the presence of  $T\beta 4$  or  $TGF\beta$  or a combination of both factors.  $T\beta 4$  addition significantly increased pSmad2 to a level comparable with  $TGF\beta$  alone, whereas combined  $T\beta 4/TGF\beta$  significantly increased pSmad2 relative to the single treatments, indicative of synergistic activation of  $TGF\beta$  signaling (A). In whole embryos from E10.5  $T\beta 4$  +/Y and -/Y embryos, levels of pSmad2 were significantly lower in both mildly and severely affected -/Y mutants compared with littermate controls (B; n=4 embryos per genotype; n=2 bands shown for mild and severe mutants), suggesting an in vivo requirement for  $T\beta 4$  to augment  $TGF\beta$  vascular signaling. Statistics: \* $P \leq 0.05$ , \*\* $P \leq 0.01$ ; 2-tailed Mann-Whitney  $U$  test. Error bars represent standard error of the mean.

hemorrhage, compared with wild-type littermates, by immunostaining for SM $\alpha$ A and phospho-Smad2 (pSmad2) with Image J quantification (Figure 8A through 8F). Consistent with the previous NG2 and SM-MHC analyses (Figure 3), the VSMC layer was significantly reduced in the mutants with hemorrhaging as compared with those with a mild, nonhemorrhagic phenotype and wild-type littermates (Figure 8A through 8D). This was accompanied by a significant reduction in both the percentage of mural cells positive for pSmad2 and intensity of pSmad2 staining within the aortic wall (Figure 8E and 8F). Interestingly, in the mildly affected  $T\beta 4$ -null mutants the percentage of pSmad2-positive cells was significantly increased as compared with the wild-type controls, suggesting some form of overcompensation to maintain the integrity of the aorta wall (Figure 8E). To provide further evidence for the ability of  $T\beta 4$  to activate the  $TGF\beta$ /Smad pathway, 10T1/2 cells were transfected with a construct encoding firefly luciferase under the control of a Smad responsive element (SRE). Treatment with  $T\beta 4$  stimulated SRE-dependent reporter activity to a level significantly higher than that of PBS alone and in combination with  $TGF\beta$  stimulated significantly higher activity than  $TGF\beta$  treatment alone (Figure 8G). Consistent with the in vivo pSmad2 data (Figure 8A through 8F) expression levels of the  $TGF\beta$  responsive genes, PAI-1, Id-1, and c-myc were found to be significantly downregulated in E10.5  $T\beta 4$  -/Y embryos compared with somite-matched  $T\beta 4$  +/Y controls, as

additional proof of defective  $TGF\beta$  downstream signaling in vivo after loss of  $T\beta 4$  (Figure 8H).

## Discussion

This study reveals that in the absence of endothelial  $T\beta 4$ , the secreted signals from the developing endothelium are no longer adequate to induce differentiation of mesodermal progenitor cells to a mural cell phenotype. At a molecular level, this is due to a deficiency in  $TGF\beta$  signaling in the mesodermal progenitor cell population and manifests as impaired mural investiture of the developing systemic vasculature in general and the aorta in particular.

We initially mapped the vascular expression of  $T\beta 4$  predominantly to the developing endothelium. Global knock-out of the  $T\beta 4$  gene in the developing embryo resulted in a proportion of the resulting E10.5 embryos exhibiting pericardial and coelomic cavity hemorrhage. An explanation for this hemorrhagic phenotype was evident through the observation that dorsal aortas in the  $T\beta 4$ -null mice had reduced mural cell coverage in comparison to control littermates. The phenotype of the global knockout embryos was incompletely penetrant and subject to apparent compensation, such that we observed mutant embryos with both intact vasculature and those with a more severe hemorrhagic phenotype. This was reflected in survival rates across distinct stages in development. Lethality occurred both between E10.5 and E14.5 due to hemorrhaging, and beyond E14.5 up to birth whereby global knockout embryos revealed epicardium-derived coronary vascular de-

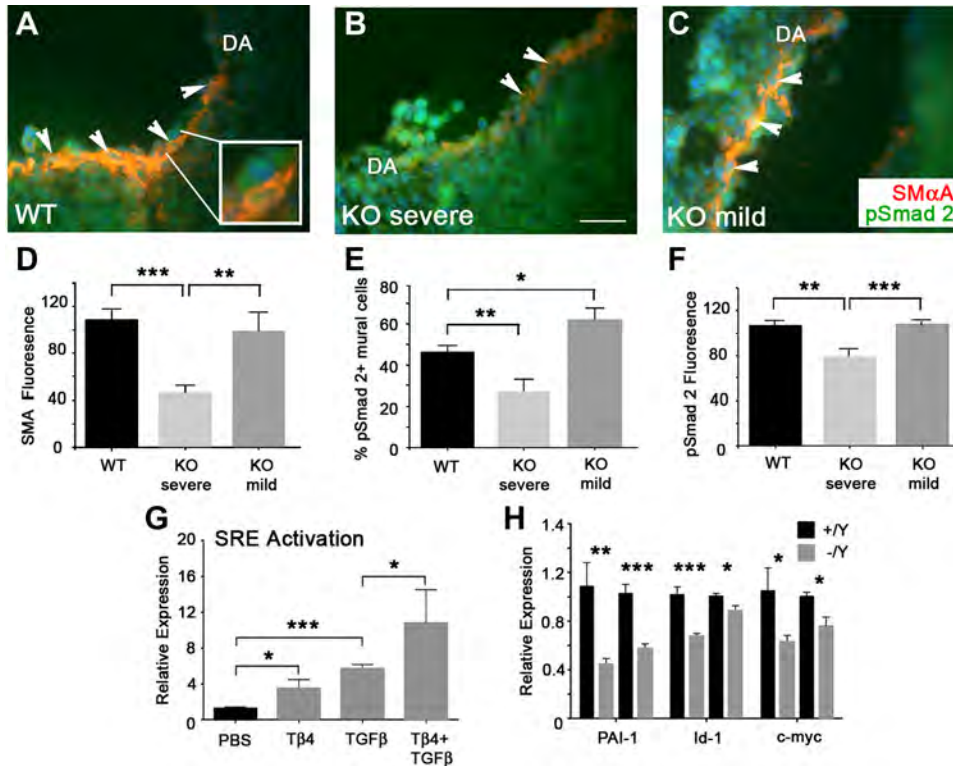


**Figure 8. TGF $\beta$  signaling is reduced in T $\beta$ 4-null embryonic aortas and correlates with the severity of hemorrhagic phenotype.** Immunostaining for SM $\alpha$ A and pSmad2 revealed a loss of smooth muscle cell coverage and corresponding reduced TGF $\beta$  signaling in the aortas of severely affected (KO severe) T $\beta$ 4  $-/\gamma$  embryos at E10.5, which exhibited hemorrhaging compared with both  $+/\gamma$  wild-type and T $\beta$ 4  $-/\gamma$  mutants that had a mild phenotype and intact vasculature (KO mild; **A** through **C**). Inset in **A** highlights punctate pSmad2 staining in the nuclei of a smooth muscle cell and underlying endothelial cell within the aorta wall; white arrowheads (**A** through **C**) highlight pSmad2-positive nuclei. The reduced mural cell coverage and pSmad2 signal was quantified using Image J to record relative fluorescence of SM $\alpha$ A. The percentage of pSmad2-positive nuclei and pSmad2 fluores-

cence in images across the 3 categories were recorded at the same filter and light intensity settings and exposure time (**D** and **E**). SM $\alpha$ A fluorescence was significantly reduced in the severe KO mutant aortas compared with both wild-type and mild mutants (**D**). The percentage of pSmad2-positive nuclei within the mural cell layer was significantly reduced in the severe mutants, whereas in the mild mutants, the percentage was significantly increased compared with wild-type indicative of a compensatory response to upregulate TGF $\beta$  signaling and maintain the integrity of the aorta wall (**E**). pSmad2 fluorescence was significantly reduced in the severe KO compared with both wild-type and compensated mutants (**F**). To confirm a synergistic effect of T $\beta$ 4 on TGF $\beta$  signaling, treatment of 10T1/2 cells transfected with a luciferase reporter construct under control of a Smad-responsive element (SRE) with 100 ng/mL T $\beta$ 4 showed a significant increase in luciferase activity compared with treatment with PBS. Treatment with 2 ng/mL TGF $\beta$  activated luciferase expression higher than T $\beta$ 4 alone, whereas a combination of both T $\beta$ 4 and TGF $\beta$  at the same doses revealed a significant additive effect on luciferase activity (**G**;  $n=6$  per treatment group). TGF $\beta$ -responsive transcription factors PAI-1, Id-1, and c-myc were significantly decreased in T $\beta$ 4  $-/\gamma$  embryos in comparison to somite matched T $\beta$ 4  $+/\gamma$  controls as measured by qRT-PCR (**H**;  $n=8$  embryo pairs run in triplicate per qRT-PCR run). DA indicates dorsal aorta. Scale bar in **B** as applies to **A** through **C**, 10  $\mu$ m. Statistics:  $*P\leq 0.05$ ,  $**P\leq 0.01$ ,  $***P\leq 0.001$ ; Student  $t$  test (**D** and **E**); 2-tailed Mann-Whitney  $U$  test (**G** and **H**). Error bars represent standard error of the mean.

facts, as previously described after shRNA knockdown of T $\beta$ 4 in the developing myocardium.<sup>9</sup> Interestingly, survival of T $\beta$ 4 global knockout mice was in stark contrast to the lethality observed between E14.5 to 16.5 after optimal cardiac-specific knockdown.<sup>9</sup> The previous RNAi model revealed a direct correlation between the severity of defective coronary angiogenesis and level of T $\beta$ 4 protein, and, moreover, reciprocal T $\beta$ 4 gain of function precisely restored the epicardial-derived vascular cell migration and differentiation disrupted by shRNA-induced loss of function. Thus we excluded, to all intents and purposes, the possibility of off-target effects, as can be associated with shRNA gene silencing, increasing the incidence of embryonic lethality. Rather, the differences between our global knockout and knockdown model are probably attributed to the fact that RNAi targeting in vivo, when sufficiently optimal to abrogate expression of the target gene, can result in a more severe phenotype than a corresponding global-null. Genetic ablation via homologous recombination through the germline, leading to complete loss of function from the outset in development, may be partially compensated for by functional orthologues,

whereas RNAi-mediated efficient knockdown, occurring rapidly and at a defined developmental stage, may not be permissive for compensation.<sup>23</sup> In a recent study, T $\beta$ 4 was described as dispensable for murine cardiac development and function after both global and cardiac-specific knockout.<sup>24</sup> This contrasts with our findings describing partially penetrant vascular phenotypes after complete loss of T $\beta$ 4; however, we acknowledge that over successive generations the incidence of embryonic lethality decreased from 40% at the outset of the study (60% survival) to a current level of 20% loss in utero (80% survival) due to presumptive modifier effects. That said, there is a clear vascular phenotype in our T $\beta$ 4-null background both within the developing systemic and coronary vasculature, and therefore differences between our findings herein and that previously described may reflect allelic variation in the targeting strategy or genetic background-dependent events. It should be noted, however, that in the earlier study, the T $\beta$ 4 knockout aortas had an apparent reduction in  $\alpha$ -SMA+ cell coverage within the vessel wall relative to wild-type controls at E14.5<sup>24</sup>; while not commented at the time, this finding is consistent with our phenotype as described.

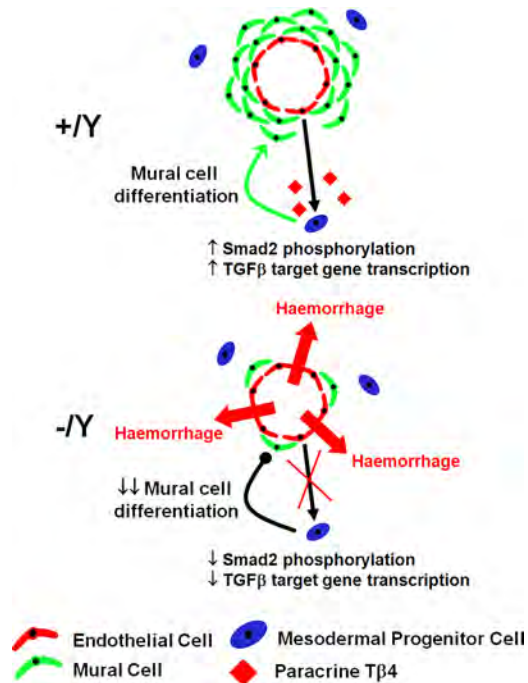


**Figure 9. Developmental model for the role of  $T\beta 4$  in the embryonic vasculature.**  $T\beta 4$  is secreted by the developing endothelium to act on mesodermal progenitor cells and stimulate  $TGF\beta$  target gene transcription through a cooperational effect on Smad2 phosphorylation with  $TGF\beta$  ligand. This results in increased transcription of canonical mural cell genes such as  $SM\alpha A$ , NG2, endosialin, and others, which in turn promotes mural cell differentiation and investiture of the endothelium with a fully formed media wall. In the absence of  $T\beta 4$ , the effect of endothelial secreted  $TGF\beta$  is reduced, leading to decreased Smad2 phosphorylation in mesodermal progenitors resulting in lower  $TGF\beta$  target gene activation. This causes impaired mural cell differentiation and reduced mural cell recruitment to the developing vessel wall. If mural cell coverage falls below a critical threshold, the vessel loses structural integrity and hemorrhage results.

Embryonic mural cell defects generally arise as a result of perturbation of one or more of the proliferation, survival, migration, or differentiation of mural cells.<sup>3</sup> A proliferation defect was ruled out on the basis of examination of E10.5 dorsal aorta mural cells for the presence of the proliferative marker phospho histone H3 and apoptosis excluded by a lack of cleaved caspase 3 expression. The anatomic location of mural cell defects also provided a clue to the role of  $T\beta 4$ . The mural cell investiture of the postnatal retina is thought to rely on the migration of phenotypically mature mural cells, along a vascular plexus.<sup>2,5</sup> As no defects were observed in the postnatal retina of  $T\beta 4$   $-/Y$  mice, it is unlikely that  $T\beta 4$  is exerting its effects by reducing the migration of mural cells to their target locations. In contrast, the vascular defects in the  $T\beta 4$   $-/Y$  mouse tend to occur in vessels which derive their mural cell coverage from the in situ differentiation of overlying mesoderm, notably the E10.5 dorsal aorta and the E14.5 dermal vasculature. Given that the normal induction of a mural cell layer around the dorsal aorta occurs over a narrow time window in murine development, between E9.5 and E10.5, and that  $T\beta 4$   $-/Y$  mice first exhibit mural cell defects at E10.5, we hypothesized that the process of mural cell

differentiation is aberrant in  $T\beta 4$   $-/Y$  mice. Further insight into the cellular basis of  $T\beta 4$ -induced mural cell differentiation arose from the observation that endothelial cell (EC)-specific  $T\beta 4$  knockdown recapitulated the aortic mural cell defects observed in the global knockout. In this instance, despite overlap in the mural cell phenotype, the embryonic lethality was not as significant as in the global knockout at stages between E10.5 and E14.5, reflecting reduced systemic vessel hemorrhaging due to incomplete knockdown of  $T\beta 4$ . Beyond E14.5, through to birth, the EC knockdown of  $T\beta 4$  had no effect on the coronary vasculature, the cause of later onset lethality in the global knockout embryos. Importantly, a reduction in mural cell differentiation after EC-specific knockdown in this study was complemented by mural cell differentiation from mesodermal progenitors on  $T\beta 4$  treatment, further supporting the specificity of the particular shRNA used in the EC targeting, identical to that previously described for the myocardial knockdown and defective coronary vasculature.<sup>9</sup>

Thus,  $T\beta 4$ , produced by the developing endothelium, acts in a paracrine fashion to stimulate the differentiation of overlying mesoderm into mature mural cells for vascular support. In support of this, exogenous administration of  $T\beta 4$  to an in vitro cell model of mural cell differentiation caused the induction of mature mural cell markers and  $T\beta 4$ -neutralizing antibody in coculture experiments prevented HUVEC-induced differentiation of A404 mural progenitors. Bioinformatic analysis of gene expression data in the  $T\beta 4$   $-/Y$  embryos implicated the  $TGF\beta$  pathway as a molecular mediator of the defects observed in the  $T\beta 4$   $-/Y$  mice. During embryogenesis,  $TGF\beta$  has been identified as one of the central factors in the formation of a normal mural cell component of the vessel wall,<sup>3</sup> and in this study, we implicate  $TGF\beta$  signaling as an important modulator of  $T\beta 4$  function in the developing vasculature. Exogenous  $T\beta 4$  was observed to upregulate the expression of  $TGF\beta$  target genes during  $T\beta 4$ -induced A404 mural cell differentiation. Moreover,  $T\beta 4$  was able to stimulate the activity of a Smad-responsive transcriptional element in transfected 10T1/2 cells and induce higher levels of phosphorylation of Smad2 when used in combination with  $TGF\beta$  than with  $TGF\beta$  alone. In vivo expression profiling of E10.5  $T\beta 4$   $-/Y$  embryos revealed a global downregulation of the  $TGF\beta$  pathway in the absence of  $T\beta 4$ , and importantly, within the mural cell and VSMC layers of E10.5  $T\beta 4$  mutant aortas, we observed correlative changes in  $TGF\beta$  signaling via immunostaining for phospho-Smad2 with severity and penetrance of the  $T\beta 4$ -mutant phenotype. In those  $T\beta 4$   $-/Y$  embryos whose vasculature appeared phenotypically normal, we observed a compensatory increase in phospho-Smad2 expression, which may underlie the incomplete penetrance of the vascular phenotype after loss of  $T\beta 4$ , whereas in the mutants with reduced mural cells and, accompanying hemorrhage, phospho-Smad2 was reduced in the VSMC layer. The implication of signaling downstream of  $TGF\beta$  in this instance is consistent with a recent study which conditionally inactivated  $TGF\beta$  type II receptor to reveal an essential role in the VSMC differentiation of the descending aorta such that mutant embryos displayed occasional aneurysms.<sup>25</sup>

We previously observed that in the developing heart, T $\beta$ 4 acts as a secreted myocardial factor on the migration and differentiation of epicardium-derived progenitor cells to form the smooth muscle layer of the coronary vasculature.<sup>9</sup> More recently, we have also shown that T $\beta$ 4 is a key transcriptional target of the basic helix-loop-helix transcription factor Hand1 and its downregulation is, in part, responsible for the defects seen in the yolk sac vasculature of *Hand1*-null mutants.<sup>26</sup> The present study allows us to expand the role of T $\beta$ 4 acting in these highly stereotyped situations to a more generalized function in vascular development. T $\beta$ 4 is a significant regulator of VSMC development, functioning as a paracrine signal from myocardial,<sup>9</sup> extra-embryonic mesodermal,<sup>26</sup> and endothelial lineages (herein), in an analogous manner to components of the Notch pathway.<sup>27</sup> Thus, T $\beta$ 4 occupies a central role in the formation of a functional circulatory system such that absence or perturbation in T $\beta$ 4 function leads to serious deleterious consequences for the growth and stability of blood vessels.

The significance of T $\beta$ 4-dependent abnormalities in vascular development is their potential relevance to adult health and disease. Many pathological processes are caused by, or involve, the subversion of normal mural cell development,<sup>28</sup> and an insult that results in depletion of medial VSMCs or a loss of functional VSMCs may be critical for adult aortic stability and vascular function. The model we propose (Figure 9) highlights the importance of secreted paracrine factors acting on mural cells and their progenitor populations, specifically in terms of their functional developmental role. Interest in identifying novel candidate molecules that function in these developmental pathways stems from the ability to agonize or antagonize their effects for therapeutic benefit. Thus, our discovery of T $\beta$ 4 as a secreted endothelial factor, which stimulates mesodermal progenitor differentiation into mural cells, can be seen in the context of not only a critical role in vascular development but highlights T $\beta$ 4 as a possible mediator of postnatal aortic function.

### Acknowledgments

We thank Shalini Jadeja and Marcus Fruttiger (UCL Institute of Ophthalmology) for technical assistance with the postnatal retina studies; RegenerX Biopharmaceuticals Inc, Rockville, MD (<http://www.regenerx.com>) for provision of clinical grade thymosin  $\beta$ 4; and Nick Henriquez (UCL Institute of Neurology) for assistance in processing microarray data.

### Sources of Funding

This work was supported by a British Heart Foundation MB PhD studentship (to A.R.).

### Disclosures

None.

### References

- Carmeliet P. Angiogenesis in health and disease. *Nat Med*. 2003;9:653–660.
- Armulik A, Abramsson A, Betsholtz C. Endothelial/pericyte interactions. *Circ Res*. 2005;97:512–523.
- Gaengel K, Genove G, Armulik A, Betsholtz C. Endothelial-mural cell signaling in vascular development and angiogenesis. *Arterioscler Thromb Vasc Biol*. 2009;29:630–638.
- von TD, Armulik A, Betsholtz C. Pericytes and vascular stability. *Exp Cell Res*. 2006;312:623–629.
- Stenzel D, Nye E, Nisancioglu M, Adams RH, Yamaguchi Y, Gerhardt H. Peripheral mural cell recruitment requires cell-autonomous heparan sulfate. *Blood*. 2009;114:915–924.
- Seki T, Hong KH, Oh SP. Nonoverlapping expression patterns of ALK1 and ALK5 reveal distinct roles of each receptor in vascular development. *Lab Invest*. 2006;86:116–129.
- Goldstein AL, Hannappel E, Kleinman HK. Thymosin beta4: actin-sequestering protein moonlights to repair injured tissues. *Trends Mol Med*. 2005;11:421–429.
- Bock-Marquette I, Saxena A, White MD, Dimaio JM, Srivastava D. Thymosin beta4 activates integrin-linked kinase and promotes cardiac cell migration, survival and cardiac repair. *Nature*. 2004;432:466–472.
- Smart N, Risebro CA, Melville AA, Moses K, Schwartz RJ, Chien KR, Riley PR. Thymosin beta4 induces adult epicardial progenitor mobilization and neovascularization. *Nature*. 2007;445:177–182.
- Smart N, Bollini S, Dube KN, Vieira JM, Zhou B, Davidson S, Yellon D, Riegler J, Price AN, Lythgoe MF, Pu WT, Riley PR. De novo cardiomyocytes from within the activated adult heart after injury. *Nature*. 2011;474:640–644.
- Grant DS, Rose W, Yaen C, Goldstein A, Martinez J, Kleinman H. Thymosin beta4 enhances endothelial cell differentiation and angiogenesis. *Angiogenesis*. 1999;3:125–135.
- Koutrafouris V, Leondiadis L, Avgoustakis K, Livanou E, Czarnecki J, Ithakissios DS, Evangelatos GP. Effect of thymosin peptides on the chick chorioallantoic membrane angiogenesis model. *Biochim Biophys Acta*. 2001;1568:60–66.
- Kisanuki YY, Hammer RE, Miyazaki J, Williams SC, Richardson JA, Yanagisawa M. Tie2-Cre transgenic mice: a new model for endothelial cell-lineage analysis in vivo. *Dev Biol*. 2001;230:230–242.
- Moses KA, DeMayo F, Braun RM, Reecy JL, Schwartz RJ. Embryonic expression of an -5/Cre gene using ROSA26 reporter mice. *Genesis*. 2001;31:176–180.
- Bourdeau A, Dumont DJ, Letarte M. A murine model of hereditary hemorrhagic telangiectasia. *J Clin Invest*. 1999;104:1343–1351.
- Foo SS, Turner CJ, Adams S, Compagni A, Aubyn D, Kogata N, Lindblom P, Shani M, Zicha D, Adams RH. Ephrin-B2 controls cell motility and adhesion during blood-vessel-wall assembly. *Cell*. 2006;124:161–173.
- Manabe I, Owens GK. Recruitment of serum response factor and hyperacetylation of histones at smooth muscle-specific regulatory regions during differentiation of a novel P19-derived in vitro smooth muscle differentiation system. *Circ Res*. 2001;88:1127–1134.
- Oshima M, Oshima H, Taketo MM. TGF-beta receptor type II deficiency results in defects of yolk sac hematopoiesis and vasculogenesis. *Dev Biol*. 1996;179:297–302.
- Untergasser G, Gander R, Lilg C, Lepperdinger G, Plas E, Berger P. Profiling molecular targets of TGF-beta1 in prostate fibroblast-to-myofibroblast transdifferentiation. *Mech Ageing Dev*. 2005;126:59–69.
- Velasco S, Alvarez-Munoz P, Pericacho M, Dijke PT, Bernabeu C, Lopez-Novoa JM, Rodriguez-Barbero A. L- and S-endoglin differentially modulate TGFbeta1 signaling mediated by ALK1 and ALK5 in L6E9 myoblasts. *J Cell Sci*. 2008;121:913–919.
- Grant DS, Kinsella JL, Kibbey MC, LaFlamme S, Burbelo PD, Goldstein AL, Kleinman HK. Matrigel induces thymosin beta 4 gene in differentiating endothelial cells. *J Cell Sci*. 1995;108:3685–3694.
- Moustakas A, Heldin CH. The regulation of TGFbeta signal transduction. *Development*. 2009;136:3699–3714.
- De Souza AT, Dai X, Spencer AG, Reppen T, Menzie A, Roesch PL, He Y, Caguyong MJ, Bloomer S, Herweijer H, Wolff JA, Hagstrom JE, Lewis DL, Linsley PS, Ulrich RG. Transcriptional and phenotypic comparisons of Ppara knockout and siRNA knockdown mice. *Nucleic Acids Res*. 2006;34:4486–4494.
- Banerjee I, Zhang J, Moore-Morris T, Lange S, Shen T, Dalton ND, Gu Y, Peterson KL, Evans SM, Chen J. Thymosin Beta 4 is dispensable for murine cardiac development and function. *Circ Res*. 2012;110:456–464.
- Langlois D, Hneino M, Bouazza L, Parlakian A, Sasaki T, Bricca G, Li JY. Conditional inactivation of TGF-beta type II receptor in smooth muscle cells and epicardium causes lethal aortic and cardiac defects. *Transgenic Res*. 2010;19:1069–1082.

26. Smart N, Dube KN, Riley PR. Identification of thymosin beta4 as an effector of Hand1-mediated vascular development. *Nat Commun*. 2010; 1:1–10.
27. Gridley T. Notch signaling in the vasculature. *Curr Top Dev Biol*. 2010; 92:277–309.
28. Lindblom P, Gerhardt H, Liebner S, Abramsson A, Enge M, Hellstrom M, Backstrom G, Fredriksson S, Landegren U, Nystrom HC, Bergstrom G, Dejana E, Ostman A, Lindahl P, Betsholtz C. Endothelial PDGF-B retention is required for proper investment of pericytes in the microvessel wall. *Genes Dev*. 2003;17:1835–1840.

## Novelty and Significance

### What Is Known?

- The stability of developing blood vessels depends on recruitment and differentiation of mural cells to support developing vascular smooth muscle cells.
- Impaired support of the vessel wall results in vascular instability and can lead to hemorrhage.
- Thymosin  $\beta 4$  ( $T\beta 4$ ) is an actin monomer-binding protein previously implicated in regulating yolk sac and coronary vessel development.

### What New Information Does This Article Contribute?

- $T\beta 4$  is required for systemic vascular development.
- An endothelial source of  $T\beta 4$  functions to maintain adequate recruitment and differentiation of mural cells/pericytes to maintain the stability of the developing aorta, cranial, and trunk vessels.
- $T\beta 4$  functions with the  $TGF\beta$  pathway to regulate mural cell development and vascular wall stability.

Vascular instability due to impaired smooth muscle support can lead to aortic aneurysm, with a worldwide prevalence of 5% among the elderly, and, due to rupture and lethal hemorrhage, is associated with a 50% to 80% mortality rate. Until now, most studies have focused on the adult pathology and existing models of the disease have identified only a limited number of causative factors. We reveal a novel congenital mouse model in which either global or endothelial-specific loss of the actin monomer-binding protein thymosin  $\beta 4$  ( $T\beta 4$ ) directly affects  $TGF\beta$ -induced vascular smooth muscle cell development, predisposing mutant vessels to wall defects ranging from lethal hemorrhage to vascular instability. Although previous studies have shown that  $T\beta 4$  plays an important role in smooth muscle contribution to extra-embryonic and coronary vascular beds, our findings reveal a more unifying function of  $T\beta 4$  in systemic vessel development per se and suggest the possibility of a new developmental paradigm for adult-onset vascular instability and aneurysm.

## Online Supplementary Material

### Online Methods

#### Mouse Lines

Mice were housed and maintained in a controlled environment and all procedures were performed in accordance with the Animals (Scientific Procedures) Act 1986, (Home Office, UK).

*Global T $\beta$ 4 KO mice.* The T $\beta$ 4 gene targeting vector was created by ligating a 6.5kb fragment containing a 5' arm (exon 1; BamHI-EcoRV) and 3' arm (exon 3; Nhe1-BamHI) flanking a neomycin resistance cassette, thereby deleting exon 2 of the *Tmsb4x* gene. The construct was linearised and electroporated into 129Sv ES cells which were subject to positive-negative selection and screening by Southern blot analysis for homologous recombination using 5' flanking and internal probes. Male chimaeras were generated from targeted ES cell lines and F1 mice generated by crossing to wild type C57Bl6/J females Progeny were genotyped using a PCR that amplifies both mutant and wild type alleles (Forward primer (intron I): 5'-GTGCTTTTGGAACTGGGAGA-3'; Reverse primer for WT intron II: 5'-AGCCCGTTCTGAAAATGG; Reverse primer for mutant, in neomycin cassette: 5'-GGCCTTCTTGACGAGTTCTT). Mice have been maintained on a C57Bl6/J background for more than 20 generations.

*Endothelial-specific T $\beta$ 4 knockdown mice.* The T $\beta$ 4 shRNA knockdown strain has been previously described (10). 23-base-pair sense and antisense T $\beta$ 4 sequences were inserted downstream of the H1 RNA pol III promoter in a modified pcDNA3 vector. Sequence of the shRNA: CTGAGATCGAGAAA TTCGATAAG; nucleotides 151–173 (Accession: NM 021278.2 *Mus musculus* thymosin  $\beta$ 4, X chromosome (*Tmsb4x*) mRNA). A 5T stop sequence, flanked by two loxP recombination sequences, was inserted upstream of the hairpin sequences to enable activation of T $\beta$ 4 knockdown by Cre recombinase. This construct was

targeted to the HPRT locus and, in order to generate endothelial-specific knockdown of T $\beta$ 4, female Tie2-Cre  $+/+$  HPRT T $\beta$ 4 shRNA  $+/-$  mice were crossed with male Tie2-Cre  $+/-$  HPRT T $\beta$ 4shRNA mice; the Tie2-Cre strain has been previously described<sup>14</sup>.

### **Antibodies**

The following antibodies were used: rabbit anti-T $\beta$ 4 (Immundiagnostik), rat anti-endomucin (eBioscience), rabbit anti-mouse SM-MHC and rabbit anti-mouse SM22 $\alpha$  (both from Abcam), rat anti-mouse PECAM and rat anti-VE-Cadherin (both from BD Pharmingen), rabbit anti-human PECAM (ProteinTech Group), rabbit anti-ZO-1 (Invitrogen) Cy3-conjugated mouse anti- $\alpha$ -SMA (Sigma), rabbit anti-NG2 (Chemicon), mouse anti-GAPDH (Chemicon), rabbit anti phospho-Smad2, rabbit anti-Smad 2 (Cell Signalling Technology). Secondary, Alexafluor conjugated antibodies were purchased from Invitrogen.

### **Recombinant Protein**

Recombinant T $\beta$ 4 was a kind gift from RegeneRx Biopharmaceuticals Inc. Recombinant TGF- $\beta$  1 was purchased from R&D systems.

### **Immunofluorescence Staining**

E10.5 embryos were fixed in 4% paraformaldehyde in PBS, embedded in OCT and cryosectioned at 10 $\mu$ m. Cryosections were washed for 10 minutes in PBS to remove OCT and then permeabilised in 0.5% Triton-X 100 for 10 minutes. After washing in PBS, sections were blocked at room temperature for 1 hour in blocking buffer (10% BSA, 10% sheep serum or 10% goat serum and 0.1% Triton-X 100 in PBS). Sections were then incubated in the primary antibody at an appropriate dilution (1:300 for Cy3-conjugated mouse anti-SMA; 1:50

for PECAM; 1:100 for all other antibodies) overnight in blocking buffer. Sections were then washed 5 times in 0.1% Triton-X 100 in PBS over the course of 1 hour. Incubation in the secondary antibody took place in blocking buffer for 1 hour at room temperature. Sections were again washed 5 times in 0.1% Triton-X 100 in PBS over the course of an hour, before mounting with coverslips using Vectashield plus DAPI. For immunofluorescence on cultured cells, cells were washed twice in PBS, fixed in 4% paraformaldehyde in PBS for 10 minutes at room temperature and stained according to the above protocol with antibodies at the following dilutions (1:250 for SM-MHC; 1:200 for SM22 $\alpha$ ; 1: 50 for PECAM).

### **Immunohistochemical Staining**

E10.5 embryo sections were prepared, as described above, except that sections were treated with 0.6% hydrogen peroxide in 80% methanol to block endogenous peroxidase activity following permeabilization. Blocking and incubation with primary antibody (1:100 anti-SM-MHC) were performed as described above. After three 10 minute washes in PBS (0.1% Triton-X 100), sections were incubated with biotinylated anti-rabbit antibody (Dako) for 1 hour at room temperature in blocking buffer. After three 10 minute washes in PBS (0.1% Triton-X 100), sections were incubated with diluted streptavidin-HRP complex (diluted in blocking buffer), washed 3 times in PBS (0.1% Triton-X 100) and developed using 3,3'-Diaminobenzidine Liquid Substrate System (Sigma). Sections were counterstained with haematoxylin, mounted with coverslips and imaged.

### **Fluorescence Imaging**

Fluorescent images were captured on an upright Zeiss Z1 fluorescent microscope or an inverted Zeiss LSM 710 confocal microscope.

## **Quantification of NG2, $\alpha$ -smooth muscle actin (SMA) and phospho-Smad2 (pSmad2)**

### **Immunofluorescence**

In order to quantify the mural cell density around embryonic E10.5, ten axial sections from each embryo providing sections throughout the length of the dorsal aorta were examined. NG2, SMA or pSmad2 immunofluorescence was imaged under constant exposure. Images were thresholded to eliminate background fluorescence. Total channel fluorescence was quantified with ImageJ software. Two perpendicular measurements of the diameter of each aortic section were averaged and used to calculate the vessel circumference. NG2 or SMA total fluorescence was then normalised to vessel circumference to produce a measure of mural cell density. The fluorescence intensity of pSmad2 positive nuclei was measured after using the ImageJ Region of Interest tool to delineate nuclei (24 nuclei per section were selected while blinded to genotype). Lumenal aortic areas were calculated using the Image J freehand selection tool and measure command, after calibrating the scale (pixels/ $\mu\text{m}$ ), according to the scale bar of the image.

### **Histological Methods**

Sections of embryos were stained with hematoxylin and eosin, using a standard protocol, mounted with coverslips and imaged.

### **Whole Mount in situ Hybridisation**

Embryos were dissected in diethyl pyrocarbonate (DEPC) treated PBS. Embryos were then fixed overnight in 4% PFA in DEPC PBS and transferred to absolute methanol for storage at  $-20^{\circ}\text{C}$ . Embryos were then rehydrated by incubating in a gradient of methanol diluted in PBT (DEPC PBS + 0.1% Tween-20). Embryos were digested in proteinase K (10 $\mu\text{g}/\text{ml}$  in PBT) at room temperature for 8-25 minutes depending on stage. Post-fixing was conducted



SMA: F – GTCCCAGACATCAGGGAGTAA  
R – TCGGATACTTCAGCGTCAGGA

SM22 $\alpha$ : F – CAACAAGGGTCCATCCTACGG,  
R – ATCTGGGCGGCCTACATCA

NG2: F – GGGCTGTGCTGTCTGTTGA  
R – TGATTCCCTTCAGGTAAGGCA

Endosialin: F – CAACGGGCTGCTATGGATTG  
R – GCAGAGGTAGCCATCGACAG

CD13: F – ATGGAAGGAGGCGTCAAGAAA  
R – CGGATAGGGCTTGGACTCTTT

Ang1: F – CACATAGGGTGCAGCAACCA  
R – CGTCGTGTTCTGGAAGAATGA

Desmin: F – GTGGATGCAGCCACTCTAGC  
R – TTAGCCGCGATGGTCTCATAC

PAI-1: F – TTCAGCCCTTGCTTGCCTC  
R – ACACTTTTACTCCGAAGTCGGT

Id-1: F – CCTAGCTGTTCGCTGAAG  
R – CTCCGACAGACCAAGTACCAC

c-myc: F – ATGCCCCTCAACGTGAACTTC  
R – CGCAACATAGGATGGAGAGCA

### **Quantification of Haemorrhage at E14.5**

E14.5 embryos were harvested from female T $\beta$ 4 +/- mice crossed with T $\beta$ 4 -/Y males. Immediately after dissection, the amount of surface haemorrhage visible under a dissection stereomicroscope was quantified according to the following scheme. Score 0 – no visible

haemorrhage, 1 – some small spots of dermal haemorrhage observed in a single location, 2 – some small spots of dermal haemorrhage observed in more than one location, 3 – a large area of haemorrhage observed in one location, 4 – a large area of dermal haemorrhage (usually flank or head) observed in one location with small foci of dermal haemorrhage observed in at least one other location, 5 – more than one large area of dermal haemorrhage observed.

### **Cell Culture**

10T1/2 cells were maintained in Dulbecco's modified Eagles' medium plus Glutamax (DMEM-Gibco) supplemented with penicillin/streptomycin and 10% heat inactivated fetal calf serum. A404 cells were maintained in  $\alpha$ -modified Eagles' medium ( $\alpha$ -MEM) supplemented with 7.5% fetal bovine serum, 200mg/ $\mu$ l L-glutamine and penicillin/streptomycin. For stimulation experiments, cells were plated at 50,000 per well in a 6 well plate and maintained in complete medium. They were treated for 4 days with either a control volume of PBS, 1 $\mu$ g/ml T $\beta$ 4, 2ng/ml TGF- $\beta$ , or 1 $\mu$ g/ml T $\beta$ 4 plus 2ng/ml TGF- $\beta$  or a neutralising rabbit polyclonal anti-T $\beta$ 4 antibody (1:250; Immundiagnostik). Each day, the medium was changed and the cells re-stimulated with the appropriate factors. On the fourth day, medium was aspirated, cells washed briefly with PBS and RNA extracted using Trizol reagent (Invitrogen). For Smad 2 phosphorylation assays, A404 cells were serum starved in 0.5% fetal calf serum in  $\alpha$ -MEM containing 200mg/ $\mu$ l L-glutamine and penicillin/streptomycin (Gibco) overnight. The following day, cells were stimulated with 1 $\mu$ g/ml T $\beta$ 4, 2ng/ml TGF- $\beta$ , or 1 $\mu$ g/ml T $\beta$ 4 plus 2ng/ml TGF- $\beta$  or a control volume of PBS. Cells were stimulated for 20 minutes. Following stimulation, medium was aspirated and cells briefly washed in PBS prior to protein extraction.

### **A404: HUVEC Co-culture**

Early passage human umbilical vein endothelial cells (HUVECs) were cultured in Endothelial Cell Growth Medium (PromoCell). For co-culture HUVECs were seeded at 20,000 cells per well in 6 well plates. After 24 hours, medium was replaced with 50:50 A404:HUVEC culture medium. After a further 48 hours, attached HUVECs were counted and an equal number of A404 cells were plated in each well. Thereafter, cells were co-cultured in A404 medium for four days, with or without the addition of a neutralising rabbit polyclonal anti-T $\beta$ 4 antibody (1:250; Immundiagnostik).

### **Cell Transfections**

10T1/2 cells were seeded in 24 well plates at 50,000 cells per well. The following day 1 $\mu$ g of the relevant plasmid was transfected into 10T1/2 cells with Effectene transfection reagent (Qiagen) according to the manufacturer's instructions. Smad activity luciferase reporter plasmids and appropriate positive and negative controls were purchased from SA Biosciences. Smad responsive constructs contained the Smad2/3/4 binding element AGCCAGACA. Following 16 hours of transfection, cells were serum starved by replacing the transfection medium with 0.5% FCS in DMEM + Glutamax. Cells were left overnight and the following day cells were stimulated for 6 hours in the presence of 100ng/ml T $\beta$ 4, 2ng/ml TGF- $\beta$ , 100ng/ml T $\beta$ 4 plus 2ng/ml TGF- $\beta$  or a control volume of PBS. Smad activity dependent firefly luciferase activity was then measured by means of a dual luciferase reporter assay (Promega) used according to the manufacturer's instructions. Renilla luciferase activity was also measured as a transfection efficiency control, and firefly luciferase activity expressed as a proportion on renilla luciferase activity.

### **Western Blotting**

Following stimulation, A404 cells were washed twice in PBS and protein extracted immediately by addition of hot (~90°C) Laemmli buffer (250mM Tris-Cl pH 6.8, 4% SDS, 25% glycerol, 0.1% bromophenol blue, 5%  $\beta$ -mercaptoethanol). Samples were separated on a 10% SDS-polyacrylamide gel. Proteins were transferred to a nitrocellulose membrane which was blocked for 2 hours in blocking buffer (5% milk in Tris buffered saline, pH7.5). Membranes were then incubated overnight at 4°C in primary antibody (1: 500 in blocking buffer for Smad antibodies; 1:1000 for GAPDH). Membranes were washed 3 times over the course of 40 minutes in TBS plus 0.05% Tween-20. Membranes were then incubated in the secondary antibody at concentration 1 in 1,000 in blocking buffer at room temperature for 1 hour. Afterwashing 3 times over the course of 40 minutes in TBS plus 0.05% Tween-20, protein bands were visualised by application of ECL western detection reagents (GE Healthcare). Bands were quantified using densitometry with ImageJ software.

### **Retinal Immunostaining**

P6 mouse pups were culled by cervical dislocation and the globes enucleated. Retinas were dissected from globes in 2x PBS and subsequently stored in methanol at -20C. For staining, methanol was aspirated and the retinas were fixed for 2 minutes in 4% formaldehyde. Formaldehyde was then aspirated and retinas left to block for 1 hour in retinal blocking buffer (2x PBS, 0.1% azide, 1% BSA, 3% Triton X-100, 0.5% Tween-20). Retinas were then incubated in primary antibodies at a concentration of 1 in 200 in retinal blocking buffer overnight at 4°C. The following day, retinas were washed five times in retinal blocking buffer over the course of an hour. Retinas were incubated in secondary antibody at a concentration of 1 in 200 in retina blocking buffer for 1 hour at room temperature. Retinas were again washed 5 times in retinal blocking buffer over the course of an hour in the dark at

room temperature. Retinas were post-fixed for 2 minutes in 4% formaldehyde before mounting and imaging.

### **Exon Array Analysis**

Micro-Arrays were performed on Affymetrix Mouse Exon 1.0ST arrays on both E12.5 embryos (T $\beta$ 4 +/Y and T $\beta$ 4 -/Y) and on 10-week old adult hearts (T $\beta$ 4 +/Y and T $\beta$ 4 -/Y). Raw data were processed with Affymetrix expression console software before being analysed for gene expression changes in Partek. Statistics were performed in R. The top 200 up- and downregulated genes were fed into Metacore software from Genego and the reverse pathway analysis tool used to determine the most statistically perturbed signalling pathways.

### **Statistics**

Statistical analysis was performed with Graphpad Prism software. Contingency tables were analysed by the chi squared test. Two tailed, unpaired, non-parametric T tests were used for all other statistical tests.

## Online Figure Legends

### Online Figure I. Generating a Thymosin $\beta$ 4 knockout mouse line.

$T\beta$ 4 was targeted by replacing exon 2 of the *tmsb4x* gene with a neomycin resistance cassette. A restriction map (A) of the wild type *tmsb4x* locus on the X chromosome, the targeting construct and the homologous recombinant allele. RV, EcoRV; H, HindIII; B, BamHI, S, Sall. Southern blot analysis to illustrate appropriate homologous recombination in an ES cell clone (B). Two separate probes were used: one against a 5' flanking sequence ( $T\beta$ 4 probe) and another within the neomycin selection cassette (neo probe), as shown in (A). Correct targeting was verified by the detection of genomic DNA fragments of the predicted sizes, with two separate restriction digests, EcoRV and HindIII, compared with a non-targeted WT 129/Sv ES cell line. Correctly targeted ES cells do not express *T $\beta$ 4* (C), as determined by northern blotting of mutant and WT ES cells, using a cDNA probe against the *T $\beta$ 4* coding region; *T $\beta$ 4* mRNA levels were quantified by phosphorimaging and normalised against  $\gamma$ -actin levels. A mouse line was established from the correctly targeted ES clone and progeny were genotyped using a PCR that amplifies both mutant and wild type alleles (D, upper gel panel). A PCR to amplify a fragment of the *SRY* gene is used to distinguish male and female embryos (D, lower gel panel). *T $\beta$ 4*-null embryos do not express *T $\beta$ 4*, as confirmed by qRT-PCR analysis on whole E10.5 embryos (E) and immunofluorescence (F, G) on sagittal sections of whole E10.5 embryos (F) and frontal sections of E14.5 hearts (G). Scale bars: (F), 500  $\mu$ m; (G), 200  $\mu$ m.

### Online Figure II. Dermal haemorrhage and reduced mural cell coverage in $T\beta$ 4-null embryos at E14.5

At E14.5, a proportion of T $\beta$ 4  $-/Y$  embryos show dermal vascular haemorrhage (**A**, **B**) (black arrowheads). Whilst blinded to genotype, embryos were assigned a score 0 (none) to 5 (severe global bleeding) to quantify the extent of dermal haemorrhage observed. A significant difference was seen between the haemorrhage scores of T $\beta$ 4  $+/Y$  and T $\beta$ 4  $-/Y$  embryos (**C**) (n=21 per genotype). The dermal vasculature was investigated by immunostaining of endothelium (endomucin) and mural cells (NG2). Vessels in T $\beta$ 4  $+/Y$  specimens displayed a robust coverage with NG2 positive mural cells (**D**) whereas in T $\beta$ 4  $-/Y$  specimens there was a reduction in resident mural cells with a complete absence in some sections of endothelium (**E**; white arrowheads). Scale bars: (**A**, **B**) 2mm, (**E**) 10 $\mu$ m. Statistics: \*  $p < 0.05$ ; Two-tailed Mann–Whitney U test. Error bar represents standard error of the mean (SEM).

**Online Figure III. T $\beta$ 4 global knock-out embryos which survive to E14.5 have epicardial-derived coronary vascular defects.**

Sections through E14.5 hearts from T $\beta$ 4  $+/Y$  (**A**) and  $-/Y$  (**B**) embryos immunostained for PECAM and SM $\alpha$ A to detect coronary endothelial and smooth muscle cells (SMCs), respectively, revealed vascular cells in the epicardial and sub-epicardial layer in the T $\beta$ 4  $-/Y$  mutant hearts which had failed to migrate into the underlying myocardium (**B**; highlighted by white arrowheads) and a lack of defined coronary arterioles as compared to T $\beta$ 4  $+/Y$  hearts (**A**; highlighted by white asterisks). Note also the sparse and disrupted myocardial layer in the T $\beta$ 4  $-/Y$  mutants (**B**), arising from defective coronary vessel development, consistent with that previously demonstrated following shRNA knock down of T $\beta$ 4 (Smart et al., 2007). Ep, epicardium; my, myocardium. Scale bar: (**A** as applies to **B**) 50 $\mu$ m. The defective migration of coronary vascular precursors from the epicardium into the myocardium

was both quantifiable and highly significant (**C**: density of PECAM<sup>+</sup> cells within the epicardium/subepicardium vs. myocardium; inset: ratio of myocardial:epicardial PECAM<sup>+</sup> cell density; n=7 +/Y; n=6 -/Y; Statistics \*\*\*p≤0.001 (0.0004); Student's t-test. Error bars represent standard error of the mean).

**Online Figure IV. TB4 is knocked down in the endothelium of Tie2-Cre Tβ4 shRNA embryos.**

Immunostaining for Tβ4 and PECAM confirmed knockdown of TB4 protein in the endothelium of the developing aorta in mutant Tie2-Cre Tβ4 shRNA embryos at E10.5 versus littermate controls (**A-D**). Two representative sections are shown for the control aorta (**A, C**) versus equivalent plane of sections of the mutant vessel (**B, D**). Tβ4 immunostaining alone highlighted reduced protein level in the mutant aortas (**E-H**) which was significant, as determined using Image J analysis across n=6 matched pairs of embryo sections. Statistics \*\*\*p≤0.001 (5.64995E-05). Two-tailed Mann-Whitney U test. Error bars represent standard error of the mean (SEM). DA, dorsal aorta; Scale bars: (**A-H**) 25μm.

**Online Figure V. Mural cell coverage of vessels is normal in Tβ4-null postnatal retinas**

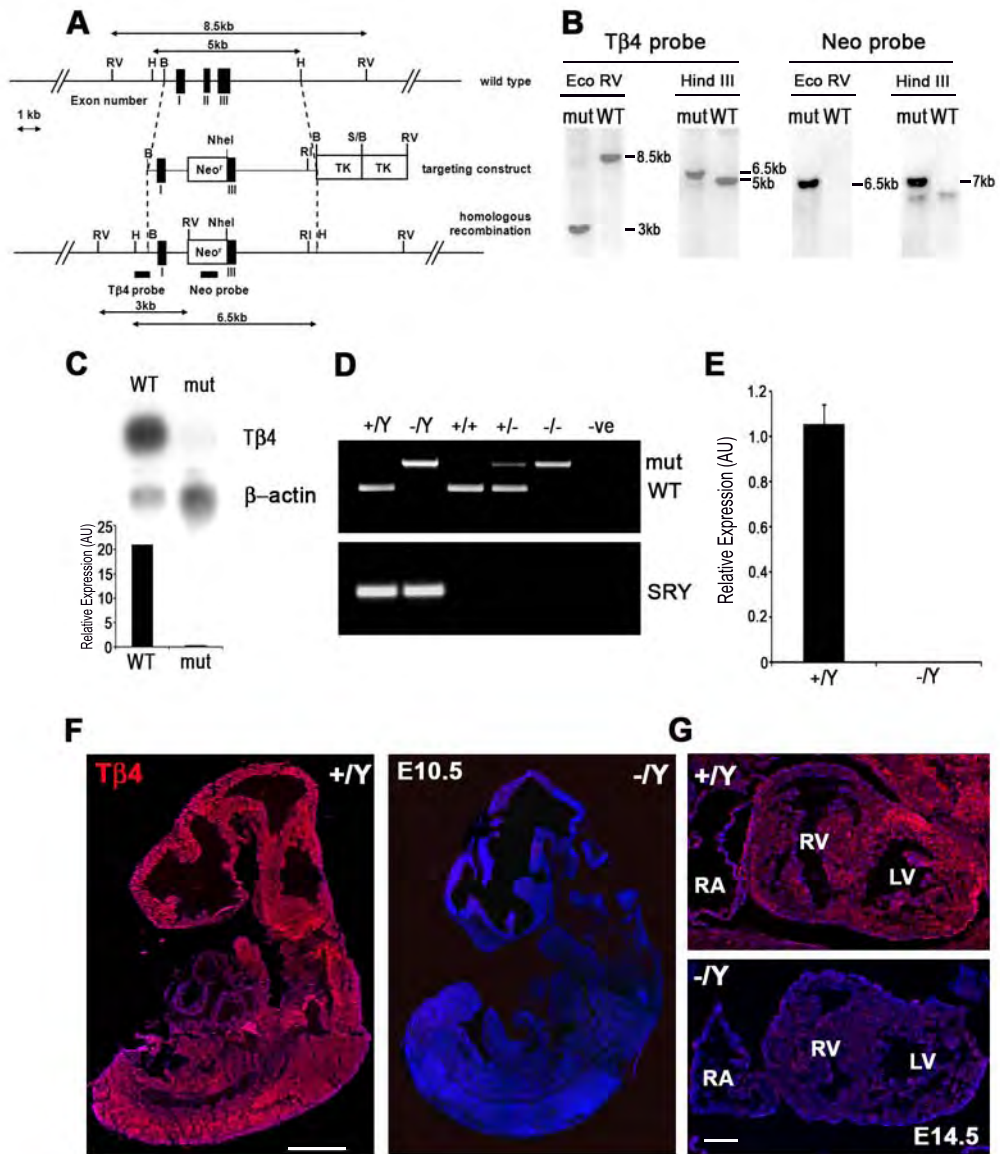
Tβ4 is expressed in the primary vascular plexus of the post-natal (P6) retina (**A, B**; red arrowheads in **A** highlight expression, and dashed line in **B** demarcates primary plexus boundary). NG2 immunostaining for isolectin b4 (Iib4) and NG2 of P6 retinas revealed no difference in the mural cell coverage of the retinal vascular primary plexus between Tβ4 -/Y animals and Tβ4 +/Y controls (**C-E**). Scale bars: (**A**)

100 $\mu$ m, (B) 50  $\mu$ m, (C, D) 50 $\mu$ m. Error bars represent the standard error of the mean (SEM).

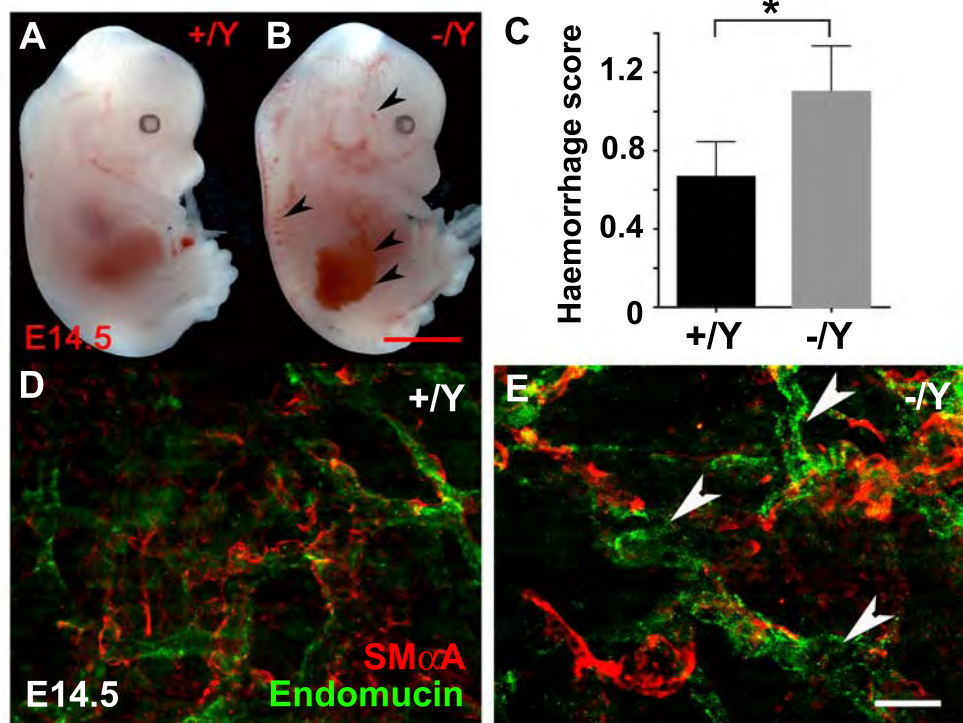
**Online Figure VI. Normal levels of apoptosis and cell proliferation in the mural cell layer of T $\beta$ 4 null dorsal aortas**

Co-immunostaining for the apoptotic marker cleaved caspase 3 (CC3) and the mural cell marker SMA revealed an absence of apoptosis in the mural cell layer of dorsal aortas in E10.5 T $\beta$ 4  $-/Y$  embryos and T $\beta$ 4  $+/Y$  controls (A, C). Punctate nuclear CC3 staining in the overlying surface epithelium of the embryo in T $\beta$ 4  $+/Y$  and T $\beta$ 4  $-/Y$  animals serve as a positive control for this staining (B, D). Similarly, co-immunofluorescence for SMA and the proliferative marker phospho-histone H3 (PHH3) demonstrated a lack of proliferation in the dorsal aorta mural cells of both T $\beta$ 4  $+/Y$  and T $\beta$ 4  $-/Y$  E10.5 embryos. PHH3 staining, in cells in the embryonic mesoderm serve as positive controls for this staining (white arrowheads) (E, F). Scale bars: (A-F) 25 $\mu$ m.

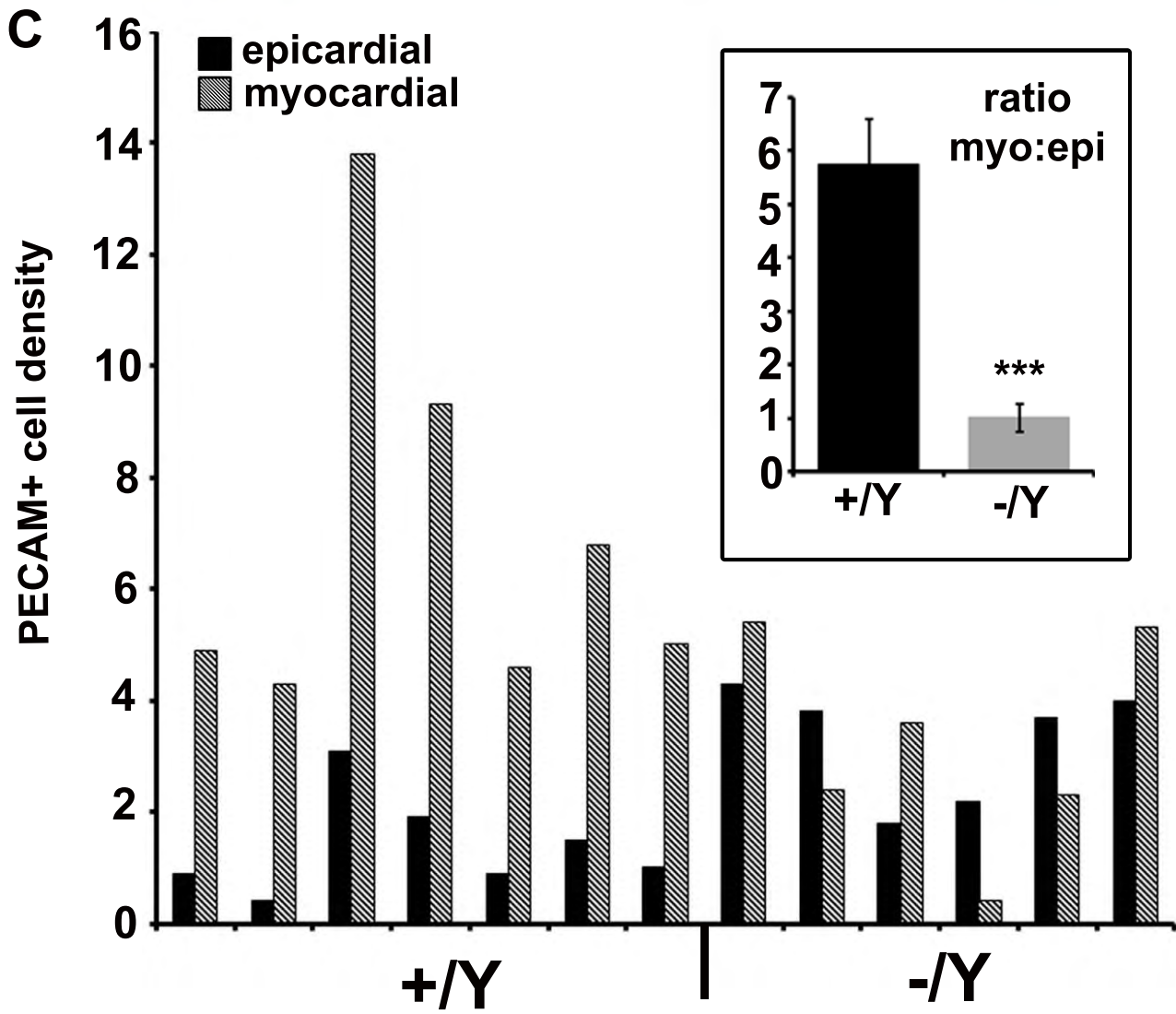
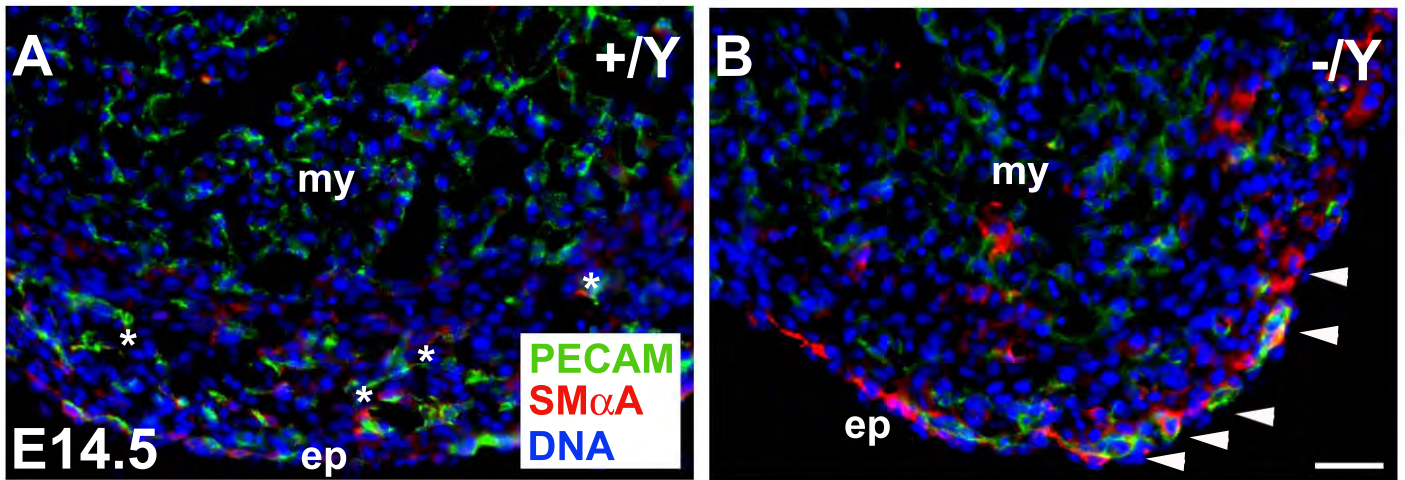
# Rossgdeutsch\_Online Fig. I



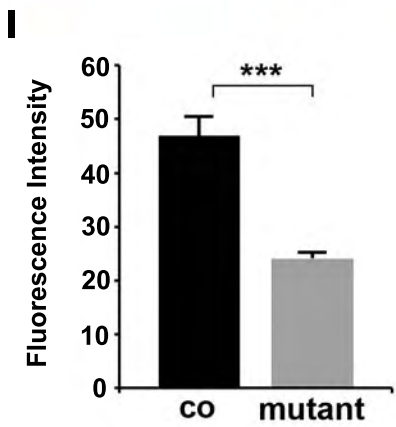
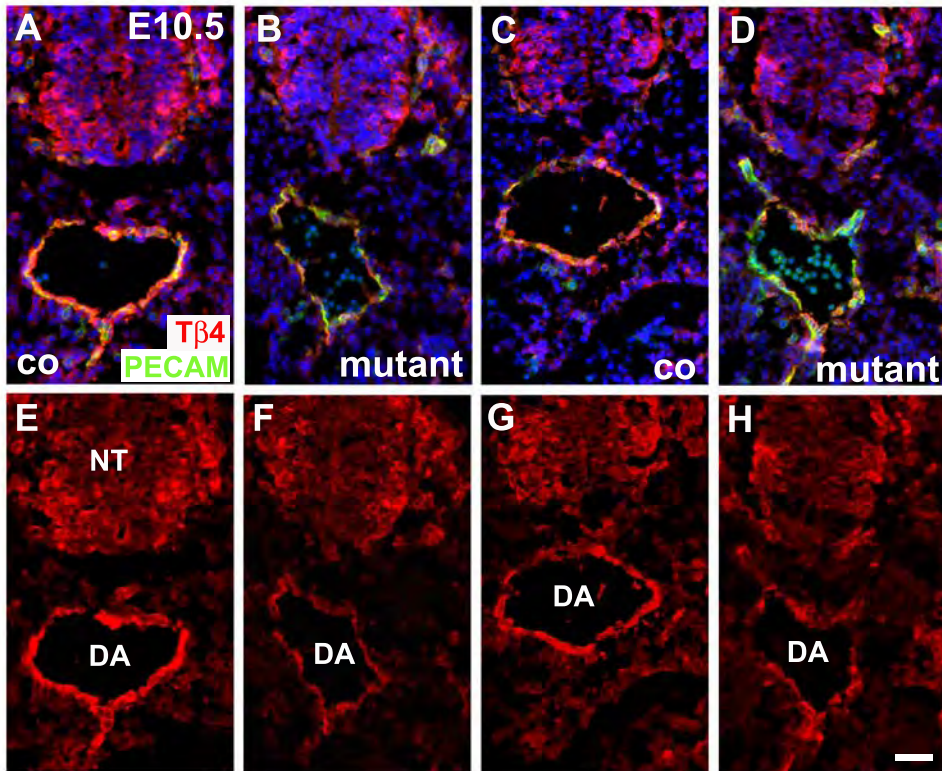
Rossgdeutsch\_Online Fig. II



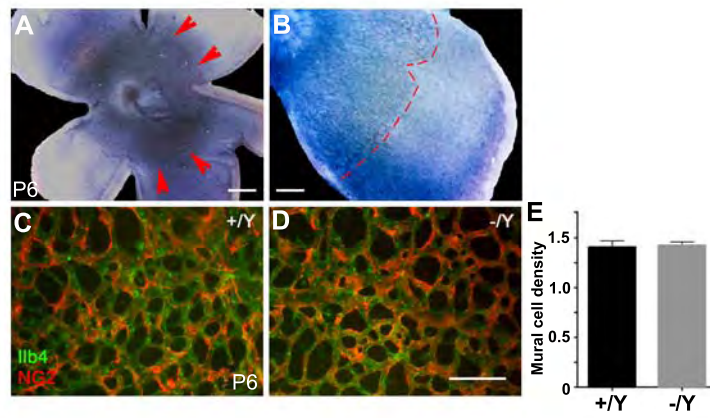
# Rossdeutsch et al\_Online Fig. III



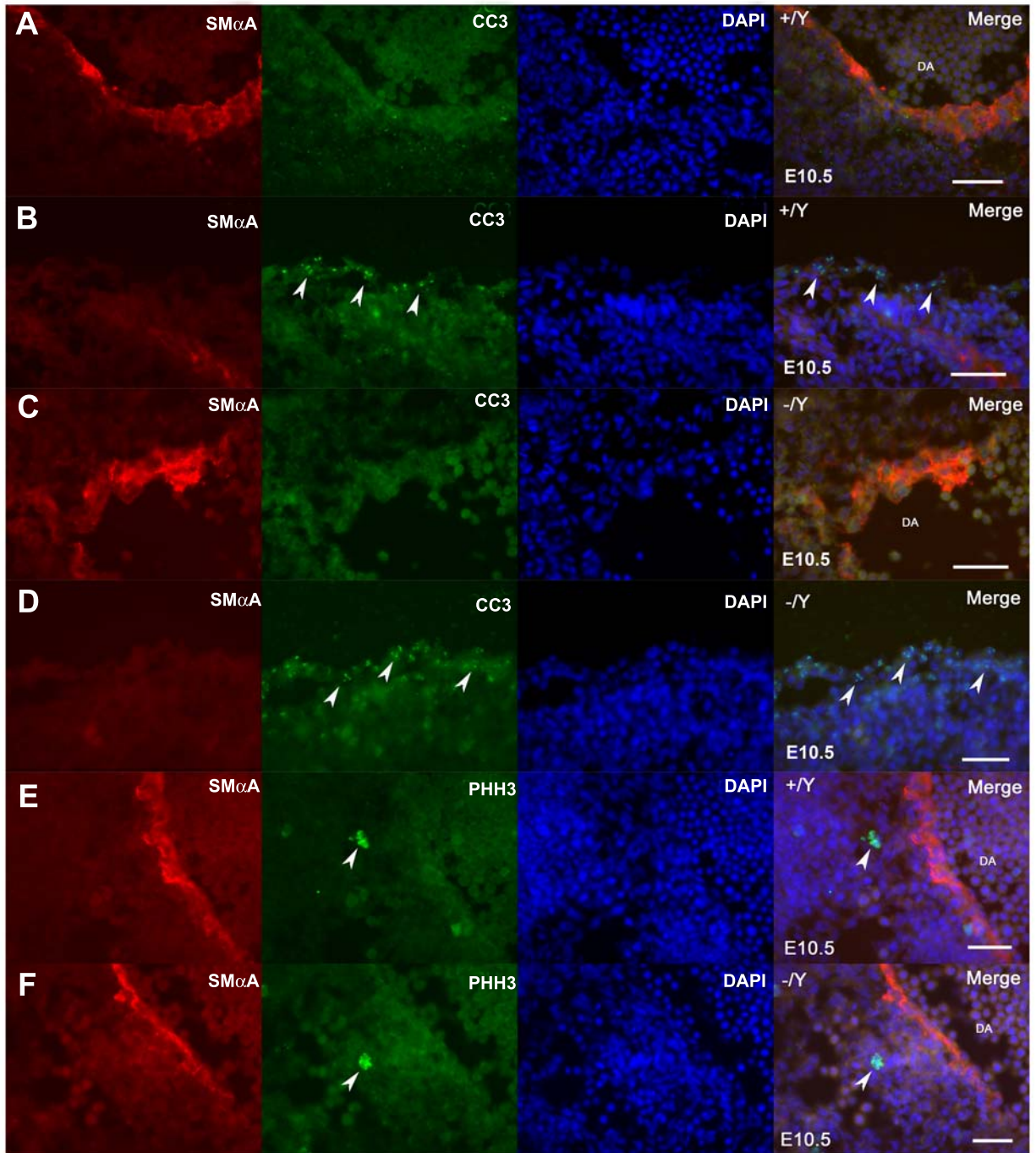
Rossdeutsch\_Online Fig. IV



Rossdeutsch\_Online Fig. V



Rossdeutsch\_Online Fig. VI



## Essential Role for Thymosin $\beta$ 4 in Regulating Vascular Smooth Muscle Cell Development and Vessel Wall Stability

Alex Rossdeutsch, Nicola Smart, Karina N. Dubé, Martin Turner and Paul R. Riley

*Circ Res.* 2012;111:e89-e102; originally published online June 20, 2012;

doi: 10.1161/CIRCRESAHA.111.259846

*Circulation Research* is published by the American Heart Association, 7272 Greenville Avenue, Dallas, TX 75231

Copyright © 2012 American Heart Association, Inc. All rights reserved.

Print ISSN: 0009-7330. Online ISSN: 1524-4571

The online version of this article, along with updated information and services, is located on the World Wide Web at:

<http://circres.ahajournals.org/content/111/4/e89>

Data Supplement (unedited) at:

<http://circres.ahajournals.org/content/suppl/2012/06/20/CIRCRESAHA.111.259846.DC1.html>

**Permissions:** Requests for permissions to reproduce figures, tables, or portions of articles originally published in *Circulation Research* can be obtained via RightsLink, a service of the Copyright Clearance Center, not the Editorial Office. Once the online version of the published article for which permission is being requested is located, click Request Permissions in the middle column of the Web page under Services. Further information about this process is available in the [Permissions and Rights Question and Answer](#) document.

**Reprints:** Information about reprints can be found online at:

<http://www.lww.com/reprints>

**Subscriptions:** Information about subscribing to *Circulation Research* is online at:

<http://circres.ahajournals.org/subscriptions/>